# Inner ear sensory system changes as extinct crocodylomorphs transitioned from land to water

Julia A. Schwab[a,1], Mark T. Young[a], James M. Neenan[b], Stig A. Walsh[a,c], Lawrence M. Witmer[d], Yanina Herrera[e], Ronan Allain[f], Christopher A. Brochu[g], Jonah N. Choiniere[h], James M. Clark[i], Kathleen N. Dollman[h,j], Steve Etches[k], Guido Fritsch[l], Paul M. Gignac[m], Alexander Ruebenstahl[n], Sven Sachs[o], Alan H. Turner[p], Patrick Vignaud[q], Eric W. Wilberg[p], Xing Xu[r], Lindsay E. Zanno[s,t], and Stephen L. Brusatte[a,c]

[a]School of GeoSciences, Grant Institute, University of Edinburgh, EH9 3FE Edinburgh, United Kingdom; [b]Oxford University Museum of Natural History, OX1 3PW Oxford, United Kingdom; [c]Department of Natural Sciences, National Museum of Scotland, EH1 1JF Edinburgh, United Kingdom; [d]Department of Biomedical Sciences, Heritage College of Osteopathic Medicine, Ohio University, Athens, OH 45701; [e]Consejo Nacional de Investigaciones Científicas y Técnicas, División Paleontología Vertebrados, Museo de La Plata, Facultad de Ciencias Naturales y Museo, National University of La Plata, B1900 La Plata, Buenos Aires, Argentina; [f]Centre de Recherche sur la Paléobiodiversité et les Paléoenvironnements, Muséum National d'Histoire Naturelle, 75005 Paris, France; [g]Department of Earth and Environmental Sciences, University of Iowa, Iowa City, IA 52242; [h]Evolutionary Studies Institute, University of the Witwatersrand, 2000 Johannesburg, South Africa; [i]Department of Biological Sciences, George Washington University, Washington, DC 20052; [j]School of Geosciences, University of the Witwatersrand, 2000 Johannesburg, South Africa; [k]Museum of Jurassic Marine Life, BH20 5PE Kimmeridge, United Kingdom; [l]Department of Reproduction Management, Leibniz Institute for Zoo and Wildlife Research, 10315 Berlin, Germany; [m]Department of Anatomy and Cell Biology, Oklahoma State University Center for Health Sciences, Tulsa, OK 74107; [n]Department of Geology and Geophysics, Yale University, New Haven, CT 06511; [o]Abteilung Geowissenschaften, Naturkunde-Museum Bielefeld, Abteilung Geowissenschaften, 33602 Bielefeld, Germany; [p]Department of Anatomical Sciences, Stony Brook University, Stony Brook, NY 11794; [q]Laboratoire de Paléontologie, Evolution, Paléoécosystèmes et Paléoprimatologie, CNRS UMR 7262, Department of Geosciences, University of Poitiers, 86073 Poitiers Cedex 9, France; [r]Key Laboratory of Vertebrate Evolution and Human Origins, Institute of Vertebrate Paleontology and Paleoanthropology, Center for Excellence in Life and Paleoenvironment, Chinese Academy of Sciences, 100044 Beijing, China; [s]Paleontology, North Carolina Museum of Natural Sciences, Raleigh, NC 27601; and [t]Department of Biological Sciences, North Carolina State University, Raleigh, NC 27695

Edited by Neil H. Shubin, University of Chicago, Chicago, IL, and approved March 10, 2020 (received for review February 4, 2020)

**Major evolutionary transitions, in which animals develop new body plans and adapt to dramatically new habitats and lifestyles, have punctuated the history of life. The origin of cetaceans from land-living mammals is among the most famous of these events. Much earlier, during the Mesozoic Era, many reptile groups also moved from land to water, but these transitions are more poorly understood. We use computed tomography to study changes in the inner ear vestibular system, involved in sensing balance and equilibrium, as one of these groups, extinct crocodile relatives called thalattosuchians, transitioned from terrestrial ancestors into pelagic (open ocean) swimmers. We find that the morphology of the vestibular system corresponds to habitat, with pelagic thalattosuchians exhibiting a more compact labyrinth with wider semicircular canal diameters and an enlarged vestibule, reminiscent of modified and miniaturized labyrinths of other marine reptiles and cetaceans. Pelagic thalattosuchians with modified inner ears were the culmination of an evolutionary trend with a long semiaquatic phase, and their pelagic vestibular systems appeared after the first changes to the postcranial skeleton that enhanced their ability to swim. This is strikingly different from cetaceans, which miniaturized their labyrinths soon after entering the water, without a prolonged semiaquatic stage. Thus, thalattosuchians and cetaceans became secondarily aquatic in different ways and at different paces, showing that there are different routes for the same type of transition.**

bony labyrinth | vestibular system | morphology | thalattosuchia | CT scanning

Throughout the history of life, there have been occasional major evolutionary transitions, in which animals developed a restyled body capable of new behaviors and adapted to new habitats. A classic example is cetaceans (whales and dolphins), which evolved from land-living mammalian ancestors into pelagic (open-ocean, sea, or shelf environment) swimmers (1). In making this shift, cetaceans followed several groups of reptiles that became secondarily aquatic much earlier, during the Mesozoic Era (2). These marine reptiles—which include plesiosauroids, pliosaurids, ichthyosaurs, mosasaurs, and extinct relatives of crocodiles and turtles—filled many of the same niches cetaceans do today (3). While the land-to-sea transition in cetaceans is captured by a sequence of fossils, whose skeletal features (4, 5) and biological and sensory abilities (6–8) have been studied in detail, far less is known about how Mesozoic reptiles moved into the water (9). This makes it difficult to address a key question: did evolution follow a similar path in modifying different groups of secondarily aquatic tetrapods for life in the open oceans?

Thalattosuchians, ancient relatives of modern crocodylians, lived during the Jurassic and Cretaceous (ca. 182–125 Ma). They are the only members of the archosaur clade—the hyperdiverse group that originated ca. 250 mya and includes birds, dinosaurs, and crocodiles—to develop fully pelagic swimming lifestyles.

## Significance

During major evolutionary transitions, groups acquire a new body plan that allows them to colonize new habitats and behave in new ways. The evolution of swimming cetaceans from land-living mammals is a prime example. We document changes to the inner ear sensory system, involved in balance and equilibrium, as extinct crocodile relatives called thalattosuchians underwent a similar transition in the Mesozoic (ca. 182–125 mya). We find that open-ocean thalattosuchians developed strikingly compact and thickened bony labyrinth after a long semiaquatic phase and after modifying their skeleton to become better swimmers. This differs from cetaceans, which miniaturized their bony labyrinths soon after entering the water. Therefore, thalattosuchians and cetaceans took different evolutionary paths from land to water.

Author contributions: J.A.S., M.T.Y., S.W., L.M.W., Y.H., and S.L.B. designed research; J.A.S. performed research; R.A., C.A.B., J.N.C., J.M.C., K.N.D., S.E., G.F., P.M.G., A.R., S.S., A.H.T., P.V., E.W.W., X.X., and L.E.Z. contributed new reagents/analytic tools; J.A.S., M.T.Y., J.M.N., S.W., L.M.W., Y.H., and S.L.B. analyzed data; and J.A.S. and S.L.B. wrote the paper.

The authors declare no competing interest.

This article is a PNAS Direct Submission.



Data deposition: The data for all 32 endosseous labyrinth models has been uploaded to Morphosource and can be accessed at https://www.morphosource.org/Detail/ProjectDetail/Show/project_id/952.

[1]To whom correspondence may be addressed. Email: julia.schwab@ed.ac.uk.

This article contains supporting information online at https://www.pnas.org/lookup/suppl/doi:10.1073/pnas.2002146117/-/DCSupplemental.

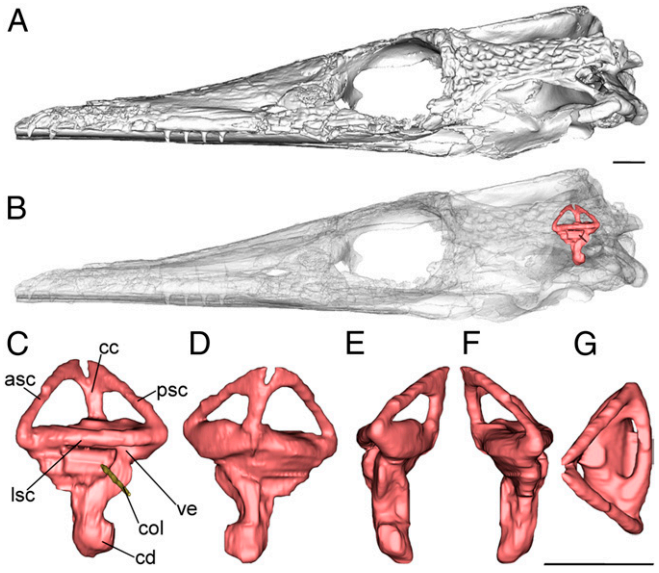


**Fig. 1.** Left bony labyrinth of the extinct thalattosuchian crocodylomorph *Pelagosaurus typus* (NHMUK PV OR 32599) based on CT data; (*A*) lateral view of the skull. (*B*) Transparent skull showing the position of the endosseous (bony) labyrinth; (*C*) lateral view; (*D*) medial view; (*E*) posterior view; (*F*) anterior view; and (*G*) dorsal view of the bony labyrinth. Abbreviations: asc, anterior semicircular canal; cc, crus commune; cd, cochlear duct; col, columella; lsc, lateral semicircular canal; psc, posterior semicircular canal; ve, vestibule. (Scale bars equal 1 cm.)

Thalattosuchians evolved from terrestrial ancestors (10), and include two main subgroups whose habitats are known from anatomical and geological evidence: semiaquatic nearshore teleosauroids, which resembled extant gharials (11), and fast-swimming open-ocean metriorhynchids, whose flippers, tail flukes, and streamlined bodies are often compared to cetaceans (3, 12, 13). Thalattosuchians are unique among marine reptiles in having their evolutionary transition documented by a series of well-preserved fossils with well-understood phylogenetic relationships, and having close living relatives (crocodylians) whose anatomy and biology can be directly observed. Thus, thalattosuchians can give critical insight into how reptiles became pelagic, and whether they underwent a similar evolutionary transformation as cetaceans.

We here study evolutionary trends in one of the most important vertebrate sensory systems—the inner ear—as thalattosuchians relocated from land to water, using high-resolution computed tomography (CT) scanning of 18 extinct species and 14 modern relatives for comparison. We focus on the endosseous labyrinth of the inner ear (Fig. 1), the bony cavity that housed the membranous sensory system. It is comprised of the vestibular system including the three semicircular ducts that detect angular acceleration and the vestibule (containing the saccule, utricle, and otolith organs) that detects linear acceleration and gravity (14). As a crucial component of the system of balance and equilibrium, bony labyrinth morphology is regularly used to reveal insights into ancient animal behavior and lifestyles (e.g., refs. 15–17). Because of the physical differences between air and water, this system should—and does—differ in terrestrial and aquatic species (18). In cetaceans, the labyrinth became highly reduced soon after they entered the water, without a long intermediate semiaquatic phase (6). One marine reptile group, pliosaurids, developed slightly smaller but more bulbous labyrinths as they changed from nearshore bottom walkers to pelagic swimmers (9). It is unclear whether other marine reptiles followed these or other evolutionary routes, which if so might speak to more general "rules" of how tetrapods become secondarily aquatic. Thalattosuchians provide a test.

## Results

Crocodylomorph semicircular canal and vestibular shape reflects ecomorphology and habitat, which are independently known for all species based on osteological and environmental evidence (Fig. 2 and *SI Appendix*, Table S2). Terrestrial species have a dorsoventrally tall labyrinth, with a particularly high anterior semicircular canal. The canal cross-sections are slender, the crus commune is narrow, and the vestibule is elongate mediolaterally. In contrast, pelagic metriorhynchids have a dorsoventrally short (compact) labyrinth. The anterior canal is only slightly higher than the posterior one, and both the crus commune and the canals have thick cross-sectional diameters. Semiaquatic teleosauroids and extant crocodylians have an intermediate labyrinth morphology, with dorsoventrally taller semicircular canals than the pelagic forms but a more compact labyrinth than the terrestrial species. These bony labyrinth shape differences between habitat groups are corroborated by numerical analyses.

Principal component analysis (PCA) of three-dimensional (3D) geometric morphometric landmarks on the semicircular canals ordinates species into a morphospace in which the first three axes describe 53.50% of overall variance (Fig. 3). The first principal component axis (PC1), explaining 22.67% of variance, represents the dorsoventral depth of the labyrinth and canal cross-sectional thickness, and segregates species by habitat. The three derived pelagic metriorhynchids (*Cricosaurus araucanensis*, *C. schroederi,* and *Torvoneustes coryphaeus*) have the most positive PC1 scores, due to their dorsoventrally compressed labyrinths and thick canals. The three terrestrial taxa (*Junggarsuchus sloani*, *Protosuchus haughtoni*, and a "sphenosuchian") have the most negative PC1 scores, because of their tall labyrinths and thin canals. Various semiaquatic taxa, including extinct teleosauroids and extant crocodylians, occupy an intermediate region between these extremes. Habitat differences are reflected to a lesser extent on PCs 2 and 3 (18.44% and 12.39% of variance, respectively).

A statistical test of morphospace occupation (PERMANOVA) upholds the observation that habitat groups form clusters, in which terrestrial, semiaquatic, and pelagic species are each significantly

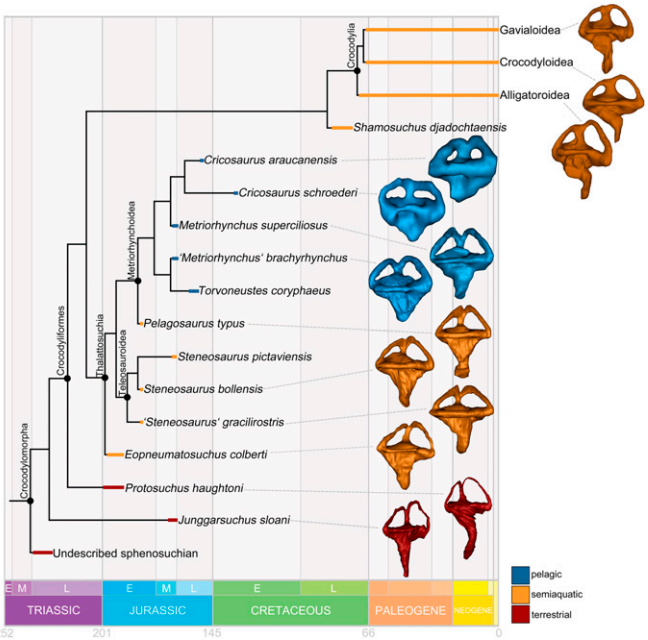


**Fig. 2.** Simplified time-scaled phylogeny showing right bony labyrinth shapes of key extinct and extant crocodylomorphs of different habitats. Labyrinths are not to scale.

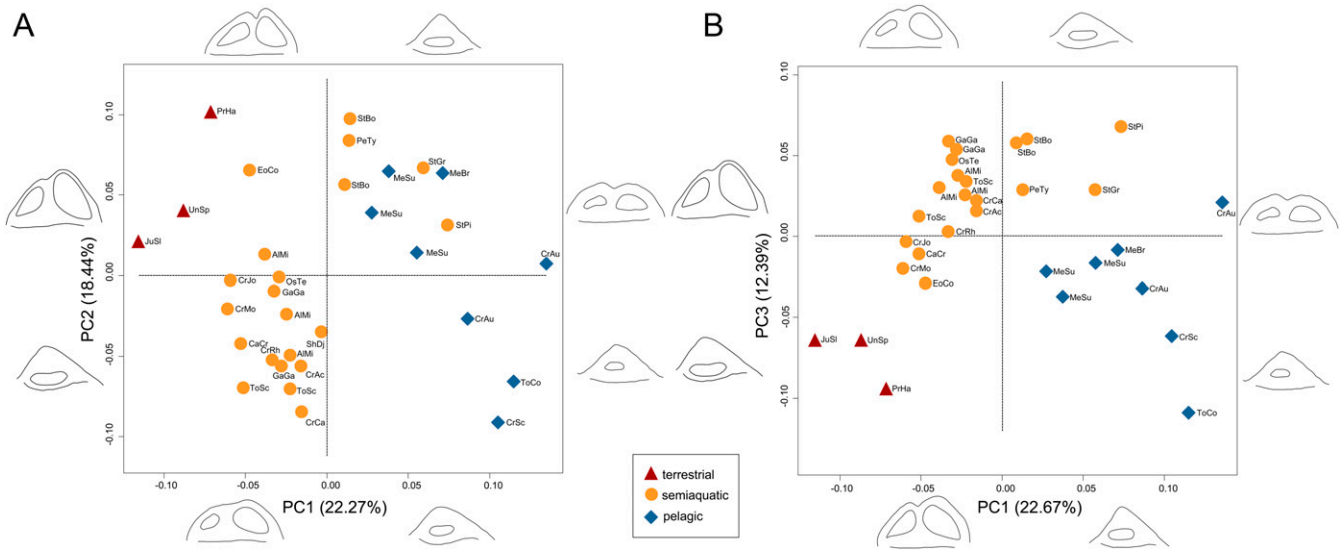


**Fig. 3.** Bony labyrinth shape morphospaces, showing the distribution of extinct and extant crocodylomorphs of different habitats, based on principal component analysis of 3D landmarks. (*A*) PC1 vs. PC2; (*B*) PC1 vs. PC3. Labyrinth outline diagrams correspond to morphological extremes at the ends of PC axes, in lateral and dorsal views. For taxa abbreviations see *SI Appendix*, Table S1.

separated from one another ($P$ value $< 0.005$; *SI Appendix*, Table S5).

A canonical variate analysis (CVA) of the PC scores demonstrates that bony labyrinth shape predicts habitat. When all crocodylomorphs are placed into habitat groupings predetermined from osteological and environmental evidence, and individual taxa are then iteratively treated as having an unknown habitat, the CVA classifies them into the correct habitat 100% of the time (Fig. 4 and *SI Appendix*, Table S6).

Because the relationship between bony labyrinth shape and habitat may be confounded by phylogeny and labyrinth size, we further explored the relationships between these variables using phylogenetic comparative methods. Pagel's lambda shows that there is a strong and significant phylogenetic signal on PC1 and PC3, whereas PC2 has a weaker but still significant signal (*SI Appendix*, Table S7). Thus, we employed phylogenetic regressions (pGLS), which found that PC1 is significantly correlated with habitat even when phylogeny is accounted for, whereas PC2 and 3 are not. PC1 remains significantly correlated with habitat in a second phylogenetic regression on size-corrected residuals, necessitated because of the significant relationship between PC1 and labyrinth size (centroid size). This is strong evidence that, regardless of phylogeny and size, the shape of the bony labyrinth is strongly correlated with habitat.

A trend is apparent when PC1—the axis most strongly correlated with habitat—is optimized onto crocodylomorph phylogeny (Fig. 5). Terrestrial species with negative PC1 scores occupy basal positions, as outgroups to the clade of thalattosuchians and extant crocodylians. On the thalattosuchian line toward pelagic metriorhynchids, the early-diverging *Eopneumatosuchus colberti*,

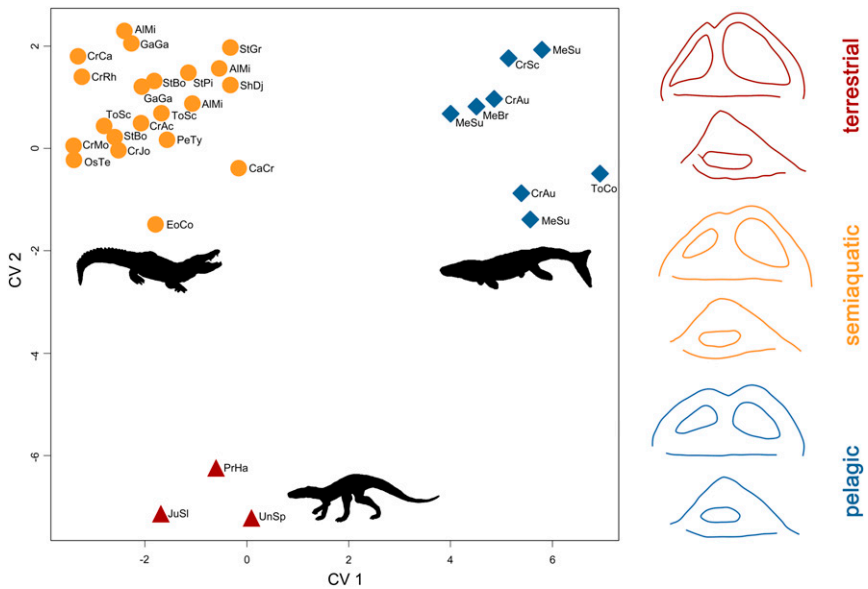


**Fig. 4.** Bony labyrinth shape morphospace, showing the distribution of extinct and extant crocodylomorphs of different habitats, based on canonical variate analysis of PC scores (Fig. 3), with mean labyrinth shapes for each habitat group, in lateral (*Top*) and dorsal (*Bottom*) views.

teleosauroids, and the basal metriorhynchoid *Pelagosaurus typus* form a grade of semiaquatic taxa with intermediate PC1 scores. PC1 scores become progressively more positive along this grade, culminating in the high PC1 scores of metriorhynchids. The most extreme labyrinth shapes, denoted by the highest PC1 scores, appear independently in two pelagic metriorhynchid subgroups: Geosaurinae (with *T. coryphaeus*) and Metriorhynchinae (with *C. schroederi* and *C. araucanensis*). Modern crocodylians exhibit a similar semiaquatic morphology as teleosauroids.

When we fit five standard models of trait evolution to PC1 scores across phylogeny, we found that an early burst model was best supported for the entire tree of extinct and extant crocodylomorphs, whereas a Brownian motion with directional trend model best fit the tree with extinct species only (*SI Appendix*, Table S10). Furthermore, when the phylogeny is plotted such that the $x$ axis is scaled to time and the $y$ axis to PC1 score, metriorhynchids/thalattosuchians are found to have higher rates of PC1 evolution than other crocodylomorphs (*SI Appendix*, Fig. S7). These results support the hypothesis that there was an evolutionary trend of increasingly specialized labyrinth shape in pelagic thalattosuchians, which involved relatively rapid rates of change compared to the background.

The cochlear duct is more challenging to characterize with landmarks than the semicircular canals, but a linear regression shows that minimum cochlear duct length correlates positively with labyrinth length. Pelagic metriorhynchids fall below the regression line, indicating that they had shorter cochlear ducts than other crocodylomorphs even when labyrinth length is held constant, which may indicate reduced hearing frequency ranges (ref. 19 and *SI Appendix*, Fig. S8).

## Discussion

We find that the shape of the crocodylomorph vestibular system corresponds to habitat, in extinct and extant species spanning more than 200 million years of evolution. There are distinct terrestrial, semiaquatic, and pelagic clusters in endosseous labyrinth morphospace, and transitions between these labyrinth types on the phylogeny. Fully pelagic Mesozoic metriorhynchids have the most transformed vestibular systems, relative to their immediate extinct semiaquatic kin, extant semiaquatic crocodylians, and terrestrial antecedents near the base of the phylogeny. In particular, metriorhynchids have a reduced, dorsoventrally shortened labyrinth with thickened semicircular canal diameters and an enlarged vestibule.

The metriorhynchid condition is reminiscent of modifications to labyrinth size and shape in other aquatic tetrapods that evolved from terrestrial ancestors. Swimming sauropterygian reptiles have smaller labyrinths than their nearshore bottom-walking relatives, and the most pelagic, fastest-swimming species (such as plesiosaurs) have compact and bulbous labyrinths with wide semicircular canal diameters, comparable to metriorhynchids like *Cricosaurus* and *Torvoneustes* (9, 20) and also sea turtles (18, 21). Cetaceans have miniaturized labyrinths, approximately 3 times smaller than terrestrial mammals of equivalent body size, although not drastically different in shape (6, 22). Aquatic mammals, like sirenians and seals, also reduced

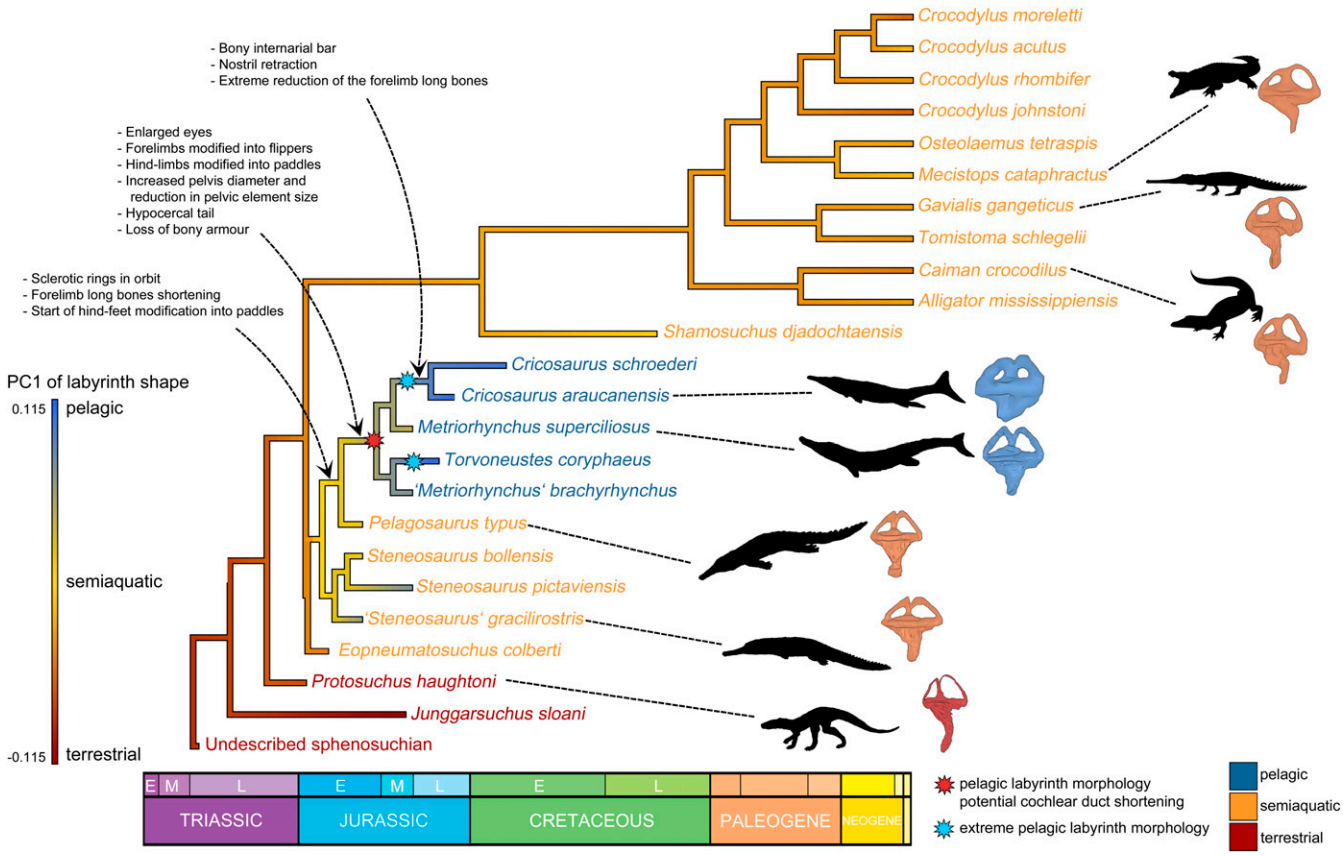


**Fig. 5.** Pelagic adaptions plotted on a time-scaled crocodylomorph phylogeny. PC1 scores of labyrinth shape, which are correlated with habitat (Figs. 3 and 4), are optimized on the phylogeny to predict ancestral states for the major clades, demonstrating a trend of increasing PC1 scores (increasingly pelagic-shaped ears) in thalattosuchians. Key cranial and postcranial features related to aquatic lifestyles are listed next to the nodes at which they appeared, based on optimizations (43). This demonstrates that thalattosuchians first developed features permitting aquatic locomotion before they developed a modified pelagic labyrinth morphology.

their canals to a lesser degree (22–24). Thus, distantly related radiations of marine reptiles independently evolved similar compact, robust, but not extremely atrophied cetaceanlike labyrinths, suggesting a general manner in which reptile vestibular sensory systems are altered for a pelagic lifestyle. More broadly, despite differences between labyrinths of pelagic reptiles and cetaceans, both exhibit labyrinth size reductions and shape modifications. This appears to be a common theme for secondarily aquatic tetrapods, transcending phylogenetic distance, tens of millions of years of time, and vastly different swimming styles (slower lateral tail undulation of reptiles vs. faster dorsoventral movements of cetaceans; ref. 25).

Similarities in labyrinth morphology indicate common physical constraints acting on agile, swimming tetrapods in the open water, but interpreting the functional significance of labyrinth size and shape changes is challenging. Longer and more arching semicircular canals are more sensitive to rotations in space (6, 26). The reduced canals of cetaceans may prevent overstimulation during exaggerated head movements associated with swimming and diving, which cannot easily be stabilized by their shortened necks (6). However, experimental evidence that extant cetaceans experience similar head accelerations as terrestrial mammals is inconsistent with this hypothesis (27). That said, it is notable that metriorhynchids, like some sauropterygians and cetaceans, have shorter necks than their close relatives (five instead of seven postaxial cervical vertebrae; refs. 11, 28), hinting that neck length may be a factor in labyrinth modifications. Perhaps the shorter neck made the head more integrated with the torso, resulting in a larger and more drag-prone head–body unit that made vestibular sensitivity less important. Alternatively, because the vestibular system is also involved in head and gaze stabilization, its reduction may reflect lesser reliance on terrestrial-style vision (compared to other senses) in pelagic species (29). Less clear is why the semicircular canals and vestibule are expanded in cross-section in metriorhynchids and other pelagic marine reptiles (9). The expansive vestibule may have housed a larger otolith, a calcium carbonate structure that is involved in perceiving linear acceleration and gravity. Large otoliths are seen in aquatic mammals such as cetaceans, sirenians, and pinnipeds (7, 22, 30), but otoliths are not visible in any of our fossil CT scans. Future work is needed to understand how bony labyrinth shape corresponds to the enclosed structures involved in sensory processing (membranous labyrinth and otoliths), and engineering techniques like computational fluid dynamics may be particularly fruitful for testing functional hypotheses (31).

The rich record of thalattosuchian fossils spanning the land-to-sea transition makes them an exemplar for illuminating evolutionary trends in secondarily aquatic reptiles, and for comparing to the well-known transitional sequence of early cetaceans. Thalattosuchians developed fully pelagic species after a long semiaquatic phase on the phylogeny, represented by the grade of close thalattosuchian outgroups, teleosauroids, and basal metriorhynchoids on the line to pelagic metriorhynchids like *Cricosaurus* and *Torvoneustes* (Fig. 5). Ancestral character state reconstructions demonstrate that this grade maintained semiaquatic labyrinth shapes along a lengthy series of internal branches, before the signature compact and bulbous pelagic labyrinths evolved in derived metriorhynchids. Pelagic labyrinths appeared after the first changes to the postcranial skeleton that allowed thalattosuchians to locomote in the water, such as shortening of the forelimbs and the modification of hindlimbs into paddles. Thus, changes to the vestibular system apparently did not lead the transition, but likely were a response to changing sensory requirements as metriorhynchids moved into deeper, more open waters. Furthermore, after the transition occurred, semiaquatic teleosauroids persisted alongside pelagic metriorhynchids for tens of millions of years (32).

Cetaceans, on the other hand, did not have such a prolonged semiaquatic phase, and the labyrinth became miniaturized rapidly as early cetaceans entered marine environments, followed by gradual changes to the postcranial skeleton associated with powerful swimming (6). The basal cetaceans that we consider most skeletally analogous to semiaquatic thalattosuchians—the nearshore remingtonocetids, which had teleosauroidlike elongate snouts, comparatively long necks, forelimbs and hindlimbs used in swimming, and robust pelves (1, 33)—had miniaturized pelagic-style labyrinths, and flourished for only a few million years. It may be that cetaceans were able to adapt more quickly to fully pelagic lifestyles, because they evolved from terrestrial ancestors that were already endothermic and gave live birth, whereas metriorhynchids had to develop these attributes after entering the water (34, 35).

Thalattosuchian crocodylomorphs are a prime example of a major evolutionary transition, and their vestibular sensory systems changed as they left the land and adapted to the water. It was a phylogenetically lengthy transition with a long semiaquatic stage, seemingly led by changes in the skeleton, related to locomotion, that allowed thalattosuchians to move in the water, followed by modifications to at least one sensory system. Key open questions, to test with future fossil discoveries and CT analyses, are how fast (in temporal terms) metriorhynchids developed a pelagic labyrinth after splitting from their semiaquatic ancestors, and how other sensory systems changed during this transition. Thalattosuchians (and other marine reptiles), like cetaceans, dramatically altered their labyrinths when becoming secondarily aquatic, but they did so in different ways and at different paces. Evolutionary transitions can start and finish in the same places, but take different routes depending on the organisms involved.

## Methods

**Dataset.** We compiled a dataset of extinct and extant crocodylomorph endosseous labyrinths, using computed-tomography scanning. Our extinct (fossil) sample (18 specimens) includes all thalattosuchians with well-preserved skulls that were accessible to us (13 specimens, including 4 teleosauroids, the basal metriorhynchoid *Pelagosaurus typus*, and 8 metriorhynchids), two basal "sphenosuchian"-grade taxa, *Protosuchus haughtoni*, *Eopneumatosuchus colberti,* and the neosuchian *Shamosuchus djadochtaensis*. These taxa span much of the evolutionary history of crocodylomorphs, from the Late Triassic to Early Cretaceous, and include a series of fossil outgroups that polarize the primitive conditions for Thalattosuchia, our main clade of interest (Fig. 2). To this dataset, we added 14 extant crocodylians for comparative purposes, including members of the 3 major extant lineages (Alligatoroidea, Crocodyloidea, and Gavialoidea) (*SI Appendix*, Table S1). Our dataset includes only adult and subadult specimens. For specimen details, see *SI Appendix*.

**Ecological Categories.** Our dataset includes species belonging to three ecomorphological or habitat groups: terrestrial, semiaquatic, and pelagic (i.e., fully aquatic). All extant crocodylians are semiaquatic, as extensive observational data show that they move between the land and nearshore aquatic habitats (36). The habitats of extinct species were assigned based on a combination of osteological and geological (environmental) data (*SI Appendix*, Table S2).

**Data Assembly.** Skulls were CT scanned at various facilities, so the scanners and scanning parameters vary (*SI Appendix*, Table S1). Some scans were sourced from the online databases Morphosource (https://www.morphosource.org/) and Digimorph (http://digimorph.org/). Bony labyrinths were segmented from the scans using Materialise Mimics 19.0 and 20.0, using the livewire and lasso tools. We segmented right labyrinths and retained them for the numerical analyses (see below); if these were not preserved, then the left labyrinth was segmented and mirrored. A recent study found no significant bilateral variation in the inner ears of wild turkeys (37), justifying this procedure. We also show that left–right asymmetry is minimal in extant crocodylians (*SI Appendix*, Figs. S9 and S10).

**Geometric Morphometric Analysis.** For each 3D rendered endosseous labyrinth model, we placed two series of semilandmarks along each of the semicircular canals, one on the internal surface and one on the external surface (*SI Appendix*, Fig. S1), using the IDAV Landmark software (38). The landmarks were digitalized using the digit.curves() function in the geomorph 3.1.2 package (39) in RStudio (40) to evenly spaced semilandmarks, 11 on the internal surface and 12 on the external surface. Landmarks on the internal surface of the canals were treated as closed structures, and those on the external surface as open structures. Subsequently, we applied Procrustes superimposition to minimize the effects of size and orientation.

**Multivariate Analyses.** We subjected the Procrustes-corrected geometric morphometric landmark dataset to principal component analysis in geomorph 3.1.2, which assimilates data from all landmarks and reduces them to a set of PC scores that summarize the labyrinth shape of each species, and allow the species to be plotted in a morphospace. We used PERMANOVA to test whether different habitat groups (terrestrial, semiaquatic, pelagic) are significantly separated from each other in the PCA morphospace using the pairwiseAdonis() function in vegan 2.5–3 (41). We calculated the mean shape for each habitat group in morphospace, along with the extreme shapes on the ends of each PC axis. We also performed a canonical variate analysis in Morpho 2.6 (42) to test the ability of the PC scores to assign individuals to known ecological categories.

**Phylogenetic Comparative Methods.** For the following phylogenetic methods, we utilized a consensus phylogeny of Crocodylomorpha based on the latest iteration of the Crocodylomorph SuperMatrix Project (43–45). The relationships of the species in our dataset are generally well resolved, but a few taxa are labile in recent phylogenetic analyses. Thus, as a sensitivity analysis, we repeated phylogenetic methods on a set of alternative phylogenies. The results were generally identical to the results gleaned from our consensus phylogeny, and we report the details in the *SI Appendix*. In all phylogenetic comparative analyses, the trees were time scaled using strap 1.4 (46) and zero-length branches were extended using the "equal" method (47).

We tested for phylogenetic signal in the PC scores with Pagel's lambda ($\lambda$), using phytools 0.6 in R (48). A $\lambda$ value close to 1.0 indicates strong phylogenetic signal, with correlation between species equal to the Brownian motion expectation that phylogeny alone can explain trait changes (49), whereas values close to zero indicate no such phylogenetic correlation between species. The $\lambda$ values are associated with a *P* value, denoting significance or nonsignificance.

We tested the correlations of labyrinth shape, labyrinth size, and habitat, using phylogenetic generalized least square regression in the R package nlme 3.1 (50), which accounts for the nonindependence of species due to phylogenetic relationships (51, 52). We performed three series of pGLS. First, we tested for correlations between raw PC scores and labyrinth size, as denoted by centroid size. Second, we tested for correlations between raw PC scores and habitat. Third, because the first pGLS found a significant relationship between labyrinth shape and size, we calculated residuals of raw PC scores vs. size, and then used the residuals in a further pGLS to test the relationship between size-corrected PC scores and habitat. We experimented with allowing the strength of phylogenetic signal ($\lambda$) to vary as a free parameter, but set $\lambda = 1.0$ (equivalent to pGLS assuming Brownian motion) because Pagel's lambda indicated a strong phylogenetic signal (see above and *SI Appendix*, Table S7).

We optimized PC scores as a continuous variable onto the phylogeny, in order to predict ancestral states for major clades and assess evolutionary trends (Fig. 5). Optimizations were performed using maximum likelihood using the fastAnc() function in phytools 0.6 (*SI Appendix*, Figs. S2–S4).

We fitted five standard models of trait evolution to the PC scores on the phylogeny: Brownian motion, Ornstein–Uhlenbeck (OU), early burst, Brownian motion with directional trend, and Lambda (Pagel). The fit of each model was assessed with maximum likelihood and the best supported model was determined by the lowest AICc score, using the R package geiger 2.0.6.2 (53). Further information on the mathematical properties of each model can be found in refs. 54–59. We recognize that interpretation of OU models can be complex and sometimes mimic other models (60), but include them here for completeness.

Testing whether certain portions of the phylogeny have variable rates of labyrinth shape evolution is challenging, because PC scores and continuous data present problems compared to discrete characters (61). To visualize rates of evolution, we used phytools 0.6 to plot a phylogeny in which the *x* axis is scaled to time and the *y* axis to PC1 value. The slopes of individual branches give an indication of which parts of the tree underwent faster or slower rates of shape evolution. We emphasize that this is a visual method and not a statistical test.

**Cochlear Duct Measurements.** We did not use 3D landmarks to quantify the shape of the cochlear duct, because the distal end is difficult to discern in CT scans, as is often not enclosed by bone. This issue also characterizes other reptile groups (21). Given these uncertainties, we favored a straightforward approach of measuring minimum cochlear duct length and using pGLS to test for correlation with specimen size. Developing a proxy for specimen size is challenging. Most of the specimens we CT scanned are skulls (often partial skulls) not associated with the postcranial bones needed to robustly estimate body mass or length. Other authors (9) have used skull length as a proxy for head size (either as a proxy for body size or to directly examine the relationship between labyrinth shape and head size), but this too is difficult for crocodylomorphs because snout length and skull proportions vary drastically within the group (62). Thus, in our cochlear duct length regression, we used the distance between the vestibules of the right and left labyrinths as a measure of specimen size, as head width is highly correlated with measures of body size in extant species (63). We realize, however, that this is a nuanced measure of specimen size, which is why we did not use it more extensively to represent specimen/head/body size to test for relationships with labyrinth size, shape, and linear measurements, as other authors have done (e.g., refs. 6 and 9).

**Data Availability.** The data for all 32 endosseous labyrinth models has been uploaded to Morphosource (https://www.morphosource.org/) and can be accessed here: https://www.morphosource.org/Detail/ProjectDetail/Show/project_id/952.

**ACKNOWLEDGMENTS.** We thank two anonymous reviewers for helpful suggestions; Olivier Lambert and Travis Park for discussion of cetaceans; Graeme Lloyd and Manabu Sakamoto for methodological advice; and Davide Foffa for statistical support. We are grateful to Susannah Maidment (Natural History Museum, London), Orestis Katsamenis (University of Southampton) and Philipp Koch (Mindener Museum, Germany) for access to their specimens. This project is supported by a Leverhulme Trust Research Project grant (RPG-2017-167) to PI S.L.B., which funds J.A.S. and M.T.Y. J.A.S. was supported by the Carl Gans Fund to attend the ICVM-19 meeting. J.M.N. is funded by a Leverhulme Trust Early Career Fellowship (ECF-2017-360). Y.H. was supported by a Humboldt Research Fellowship from the Alexander von Humboldt Foundation and the ANPCyT (PICTs 2016-0267, 2016-1039). P.M.G. was supported by a National Science Foundation grant (DEB 1754659). A.H.T. and E.W.W. were supported by a National Science Foundation grant (DEB 1754596). X.X. was supported by a National Natural Science Foundation of China grant (41688103).

1. J. Gatesy *et al.*, A phylogenetic blueprint for a modern whale. *Mol. Phylogenet. Evol.* **66**, 479–506 (2013).
2. R. Motani, The evolution of marine reptiles. *Evol. Educ. Outreach* **2**, 224–235 (2009).
3. D. Foffa, M. T. Young, T. L. Stubbs, K. G. Dexter, S. L. Brusatte, The long-term ecology and evolution of marine reptiles in a Jurassic seaway. *Nat. Ecol. Evol.* **2**, 1548–1555 (2018).
4. P. D. Gingerich, S. M. Raza, M. Arlf, M. Anwar, X. Zhou, New whale from the Eocene of Pakistan and the origin of cetacean swimming. *Nature* **368**, 844–847 (1994).
5. J. G. M. Thewissen, E. M. Williams, L. J. Roe, S. T. Hussain, Skeletons of terrestrial cetaceans and the relationship of whales to artiodactyls. *Nature* **413**, 277–281 (2001).
6. F. Spoor, S. Bajpai, S. T. Hussain, K. Kumar, J. G. M. Thewissen, Vestibular evidence for the evolution of aquatic behaviour in early cetaceans. *Nature* **417**, 163–166 (2002).
7. F. Spoor, J. G. M. Thewissen, "Comparative and functional anatomy of balance in aquatic mammals" in *Sensory Evolution on the Threshold: Adaptations in Secondarily Aquatic Vertebrates*, J. G. M. Thewissen, S. Nummela, Eds. (University of California Press, 2008), pp. 257–286.
8. E. G. Ekdale, "The ear of mammals: From monotremes to humans" in *Evolution of the Vertebrate Ear*, J. A. Clack, R. R. Fay, A. N. Popper, Eds. (Springer International Publishing, 2016), pp. 175–206.
9. J. M. Neenan *et al.*, Evolution of the sauropterygian labyrinth with increasingly pelagic lifestyles. *Curr. Biol.* **27**, 3852–3858.e3 (2017).
10. R. B. Irmis, S. J. Nesbitt, H. Sues, Early Crocodylomorpha. *Geol. Soc. Lond. Spec. Publ.* **379**, 275–302 (2013).
11. C. W. Andrews, *Descriptive Catalogue of the Marine Reptiles of the Oxford Clay: Part II* (British Museum, Natural History, London, 1913).
12. M. T. Young, S. L. Brusatte, M. Ruta, M. B. Andrade, The evolution of Metriorhynchoidea (Mesoeucrocodylia, Thalattosuchia): An integrated approach using geometrics morphometrics, analysis of disparity and biomechanics. *Zool. J. Linn. Soc.* **158**, 801–859 (2010).
13. M. T. Young, S. L. Brusatte, B. L. Beatty, M. B. De Andrade, J. B. Desojo, Tooth-on-tooth interlocking occlusion suggests macrophagy in the mesozoic marine crocodylomorph dakosaurus. *Anat. Rec. (Hoboken)* **295**, 1147–1158 (2012).

14. H. M. de Burlet, "Vergleichende anatomie des stato-akustischen organs [in German]" in *Handbuch der vergleichende Anatomie der Wirbeltiere* (Urban and Schwarzberg, Berlin, 1934), vol. 2, pp. 1293–1432.
15. C. Pfaff, T. Martin, I. Ruf, Bony labyrinth morphometry indicates locomotor adaptations in the squirrel-related clade (Rodentia, Mammalia). *Proc. Biol. Sci.* **282**, 20150744 (2015).
16. A. Palci, M. N. Hutchinson, M. W. Caldwell, M. S. Y. Lee, The morphology of the inner ear of squamate reptiles and its bearing on the origin of snakes. *R. Soc. Open Sci.* **4**, 170685 (2017).
17. J. A. Schwab, J. Kriwet, G. W. Weber, C. Pfaff, Carnivoran hunting style and phylogeny reflected in bony labyrinth morphometry. *Sci. Rep.* **9**, 70 (2019).
18. J. A. Georgi, J. S. Sipla, "Comparative and functional anatomy of balance in aquatic reptiles and birds" in *Sensory Evolution on the Threshold: Adaptations in Secondarily Aquatic Vertebrates*, J. G. M. Thewissen, S. Nummela, Eds. (University of California Press, 2008), pp. 233–256.
19. S. A. Walsh, P. M. Barrett, A. C. Milner, G. Manley, L. M. Witmer, Inner ear anatomy is a proxy for deducing auditory capability and behaviour in reptiles and birds. *Proc. Biol. Sci.* **276**, 1355–1360 (2009).
20. J. M. Neenan, T. M. Scheyer, The braincase and inner ear of *Placodus gigas* (Sauropterygia, Placodontia)—A new reconstruction based on micro-computed tomography data. *J. Vertebr. Paleontol.* **32**, 1350–1357 (2012).
21. S. Evers *et al*., Neurovascular anatomy of the protostegid turtle *Rhinochelys pulchriceps* and comparisons of membranous and endosseous labyrinth shape in an extant turtle. *Zool. J. Linn. Soc.* **20**, 1–29 (2019).
22. J. Hyrtl, *Comparative-Anatomical Studies on the Internal Auditory Organ of Humans and Mammals* [in German] (Ehrlich, Prague, 1845).
23. E. G. Ekdale, Comparative anatomy of the bony labyrinth (inner ear) of placental mammals. *PLoS One* **8**, e66624 (2013).
24. C. M. Loza, A. E. Latimer, M. R. Sánchez-Villagra, A. A. Carlini, Sensory anatomy of the most aquatic of carnivorans: The Antarctic Ross seal, and convergences with other mammals. *Biol. Lett.* **13**, 20170489 (2017).
25. J. A. Massare, Swimming capabilities of Mesozoic marine reptiles: Implications for method of predation. *Paleobiology* **12**, 187–205 (1988).
26. E. G. Ekdale, Form and function of the mammalian inner ear. *J. Anat.* **228**, 324–337 (2016).
27. B. M. Kandel, T. E. Hullar, The relationship of head movements to semicircular canal size in cetaceans. *J. Exp. Biol.* **213**, 1175–1181 (2010).
28. M. T. Young, M. B. Andrade, What is *Geosaurus*? Redescription of *Geosaurus giganteus* (Thalattosuchia: Metriorhynchidae) from the Upper Jurassic of Bayern, Germany. *Zool. J. Linn. Soc.* **157**, 551–585 (2009).
29. P. G. Cox, N. Jeffery, Morphology of the mammalian vestibulo-ocular reflex: The spatial arrangement of the human fetal semicircular canals and extraocular muscles. *J. Morphol.* **268**, 878–890 (2007).
30. A. A. Gray, "The labyrinth of the Carnivora" in *The Labyrinth of Animals: Including Mammals, Birds, Reptiles and Amphibians 1* (J. A. Churchill, London, 1907).
31. I. A. Rahman, Computational fluid dynamics as a tool for testing functional and ecological hypotheses in fossil taxa. *Palaeontology* **60**, 451–459 (2017).
32. M. T. Young, S. Sachs, Evidence of thalattosuchian crocodylomorphs in the Portland Stone Formation (Late Jurassic) of England, and a discussion on Cretaceous teleosauroids. *Hist. Biol.*, 10.1080/08912963.2019.1709453 (2020).
33. R. M. Bebej, I. S. Zalmout, A. A. Abed El-Aziz, M. S. M. Antar, P. D. Gingerich, First remingtonocetid archaeocete (Mammalia, Cetacea) from the middle Eocene of Egypt with implications for biogeography and locomotion in early cetacean evolution. *J. Paleontol.* **89**, 882–893 (2015).
34. Y. Herrera *et al*., Morphology of the sacral region and reproductive strategies of Metriorhynchidae: A counter-inductive approach. *Earth Environ. Sci. Trans. R. Soc. Edinb.* **106**, 247–255 (2017).
35. N. Séon *et al*., Thermophysiologies of Jurassic marine crocodylomorphs inferred from the oxygen isotope composition of their tooth apatite. *Philos. Trans. R. Soc. Lond. B Biol. Sci.* **375**, 20190139 (2020).
36. G. Grigg, D. Kirshner, *Biology and Evolution of Crocodylians* (CSIRO and Cornell University Press, 2015).
37. D. G. Cerio, L. M. Witmer, Intraspecific variation and symmetry of the inner-ear labyrinth in a population of wild turkeys: Implications for paleontological reconstructions. *PeerJ* **7**, e7355 (2019).
38. D. F. Wiley *et al*., *Evolutionary Morphing* (IEEE, Washington, DC, 2005), pp. 431–438.
39. D. Adams, M. Collyer, A. Kaliontzopoulou, Geomorph: Software for Geometric Morphometric Analyses. R Package Version 3.1.0. https://CRAN.R-project.org/package=geomorph. Accessed 1 April 2020.
40. R Core Team, *R: A Language and Environment for Statistical Computing*, (R Foundation for Statistical Computing, Vienna, Austria, 2018).
41. J. Oksanen, R. Kindt, B. O'Hara, vegan: Community Ecology Package. R Package Version 2.5-3. https://CRAN.R-project.org/package=vegan.
42. S. Schlager, "Morpho and Rvcg–shape analysis in R" in *Statistical Shape and Deformation Analysis*, G. Zheng, S. Li, G. Szekely, Eds. (Academic Press, 2017), pp. 217–256.
43. A. Ősi, M. T. Young, A. Galácz, M. Rabi, A new large-bodied thalattosuchian crocodyliform from the Lower Jurassic (Toarcian) of Hungary, with further evidence of the mosaic acquisition of marine adaptations in Metriorhynchoidea. *PeerJ* **6**, e4668 (2018).
44. M. M. Johnson, M. T. Young, S. L. Brusatte, Re-description of two contemporaneous mesorostrine teleosauroids (Crocodylomorpha, Thalattosuchia) from the Bathonian of England, and insights into the early evolution of Machimosaurini. *Zoo. J. Linn. Soc.*, 10.1093/zoolinnean/zlz037 (2019).
45. M. T. Young *et al*., Convergent evolution and possible constraint in the posterodorsal retraction of the external nares in pelagic crocodylomorphs. *Zool. J. Linn. Soc.*, in press.
46. M. A. Bell, G. T. Lloyd, Strap: Stratigraphic Tree Analysis for Palaeontology. R Package Version 1.4. https://CRAN.R-project.org/package=strap. Accessed 1 April 2020.
47. S. L. Brusatte, M. J. Benton, M. Ruta, G. T. Lloyd, Superiority, competition, and opportunism in the evolutionary radiation of dinosaurs. *Science* **321**, 1485–1488 (2008).
48. L. J. Revell, Phytools: An R package for phylogenetic comparative biology (and other things). *Methods Ecol. Evol.* **3**, 217–223 (2012).
49. M. Pagel, Inferring the historical patterns of biological evolution. *Nature* **401**, 877–884 (1999).
50. J. Pinheiro, D. Bates, S. DebRoy, D. Sarkar, R Core Team, nlme: Linear and Nonlinear Mixed Effects Models. R Package Version 3.1-141. https://CRAN.R-project.org/package=nlme. Accessed 1 April 2020.
51. A. Grafen, The phylogenetic regression. *Philos. Trans. R. Soc. Lond. B Biol. Sci.* **326**, 119–157 (1989).
52. F. J. Rohlf, Comparative methods for the analysis of continuous variables: Geometric interpretations. *Evolution* **55**, 2143–2160 (2001).
53. L. J. Harmon, J. T. Weir, C. D. Brock, R. E. Glor, W. Challenger, GEIGER: Investigating evolutionary radiations. *Bioinformatics* **24**, 129–131 (2008).
54. T. F. Hansen, Stabilizing selection and the comparative analysis of adaptation. *Evolution* **51**, 1341–1351 (1997).
55. B. C. O'Meara, C. Ané, M. J. Sanderson, P. C. Wainwright, Testing for different rates of continuous trait evolution using likelihood. *Evolution* **60**, 922–933 (2006).
56. G. Hunt, Measuring rates of phenotypic evolution and the inseparability of tempo and mode. *Paleobiology* **38**, 351–373 (2012).
57. G. J. Slater, L. J. Harmon, M. E. Alfaro, Integrating fossils with molecular phylogenies improves inference of trait evolution. *Evolution* **66**, 3931–3944 (2012).
58. G. J. Slater, Phylogenetic evidence for a shift in the mode of mammalian body size evolution at the Cretaceous-Palaeogene boundary. *Methods Ecol. Evol.* **4**, 734–744 (2013).
59. R. B. J. Benson, E. Starmer-Jones, R. A. Close, S. A. Walsh, Comparative analysis of vestibular ecomorphology in birds. *J. Anat.* **231**, 990–1018 (2017).
60. N. Cooper, G. H. Thomas, C. Venditti, A. Meade, R. P. Freckleton, A cautionary note on the use of Ornstein Uhlenbeck models in macroevolutionary studies. *Biol. J. Linn. Soc. Lond.* **118**, 64–77 (2016).
61. G. T. Lloyd, S. C. Wang, S. L. Brusatte, Identifying heterogeneity in rates of morphological evolution: Discrete character change in the evolution of lungfish (Sarcopterygii; Dipnoi). *Evolution* **66**, 330–348 (2012).
62. E. W. Wilberg, Investigating patterns of crocodyliform cranial disparity through the Mesozoic and Cenozoic. *Zool. J. Linn. Soc.* **181**, 189–208 (2017).
63. H. D. O'Brien *et al*., Crocodylian head width allometry and phylogenetic prediction of body size in extinct Crocodyliforms. *Integr. Organismal Biol.***1**, 1–15 (2019).

Supplementary Information for:

# Inner ear sensory system changes as extinct crocodylomorphs transitioned from land to water

Julia A. Schwab[a,*], Mark T. Young[a], James M. Neenan[b], Stig A. Walsh[a,c], Lawrence M. Witmer[d], Yanina Herrera[e], Ronan Allain[f], Christopher A. Brochu[g], Jonah N. Choiniere[h], James M. Clark[i], Kathleen N. Dollman[h,j], Steve Etches[k], Guido Fritsch[l], Paul M. Gignac[m], Alexander Ruebenstahl[n], Sven Sachs[o], Alan H. Turner[p], Patrick Vignaud[q], Eric W. Wilberg[p], Xu Xing[r], Lindsay E. Zanno[s,t] & Stephen L. Brusatte[a,c]

[a]School of GeoSciences, Grant Institute, James Hutton Road, The King's Buildings, University of Edinburgh, Edinburgh, EH9 3FE, UK; [b]Oxford University Museum of Natural History, Oxford, OX1 3PW, United Kingdom; [c] Department of Natural Sciences, National Museum of Scotland, National Museum of Scotland, Chambers Street, Edinburgh, EH 1 1JF, UK; [d]Department of Biomedical Sciences, Heritage College of Osteopathic Medicine, Ohio University, Athens, Ohio 45701, USA; [e]Consejo Nacional de Investigaciones Científicas y Técnicas, División Paleontología Vertebrados, Museo de La Plata, FCNyM, UNLPNational University of La Plata, La Plata, Argentina; [f] Centre de Recherche sur la Paléobiodiversité et les Paléoenvironnements, Muséum National d'Histoire Naturelle, CP 38, 8 rue Buffon, 75005 Paris, France; [g]Department of Earth and Environmental Sciences, University of Iowa, Iowa City, Iowa 52242, USA; [h]Evolutionary Studies Institute, University of the Witwatersrand, Johannesburg 2000, South Africa; [i]Department of Biological Sciences, George Washington University, Washington DC 20052, USA; [j]School of Geosciences, University of the Witwatersrand, Johannesburg 2000, South Africa;



www.pnas.org/cgi/doi/10.1073/pnas.2002146117

[k]Museum of Jurassic Marine Life, Kimmeridge, BH20 5PE, UK; [l]Department of Reproduction Management, Leibniz Institute for Zoo and Wildlife Research, 10315 Berlin, Germany; [m]Department of Anatomy and Cell Biology, Oklahoma State University Center for Health Sciences, Tulsa, Oklahoma 74107, USA; [n]Department of Geology and Geophysics, Yale University, New Haven, CT 06511, USA; [o]Abteilung Geowissenschaften, Naturkunde-Museum Bielefeld, Naturkunde-Museum Bielefeld, Abteilung Geowissenschaften, Adenauerplatz 2, 33602 Bielefeld, Germany; [p]Department of Anatomical Sciences, Stony Brook University, Stony Brook, New York 11794, USA; [q] Laboratoire de Paléontologie, Evolution, Paléoécosystèmes et Paléoprimatologie, CNRS UMR 7262, Department of Geosciences, University of Poitiers, France; [r]Institute of Vertebrate Paleontology & Paleoanthropology, Chinese Academy of Sciences, Beijing, China; [s]Paleontology, North Carolina Museum of Natural Sciences, Raleigh, NC 27601, USA; [t]Department of Biological Sciences, North Carolina State University, Raleigh, NC 27695, USA

* Correspondence: julia.schwab@ed.ac.uk

## 1. Specimens Examined

**Table S1.** Detailed information on the specimens we scanned; their museum specimen numbers, ages, and CT scanning parameters. The abbreviations are the notions used in the Figures in the main text and the Supplementary Tables.

| Taxa | ID | Abbr. | voxel size (mm) | facility |
|---|---|---|---|---|
| *Junggarsuchus sloani* | IVPP V14010 | JuSl | 0.13 | Institute of Vertebrate Paleontology and Paleoanthropology (IVPP) of the Chinese Academy of Sciences |
| Undescribed sphenosuchian | NCSM 21722 | UnSp | 0.039327 | Nikon XTH 225 ST µCT scanner, Shared Materials Instrumentation Facility, Duke University, Durham, NC |
| *Eopneumatosuchus colberti* | MNA V2460 | EoCo | 0.092 | General Electric eXplore Locus in vivo Small Animal µCT scanner, Ohio University µCT Scanning Facility |
| *Protosuchus haughtoni* | BP/1/4770 | PrHa | 0.0538 | Nikon Metrology XTH 225/320 LC dual source industrial CT system, University of the Witwatersrand, Johannesburg |
| *'Steneosaurus' cf. gracilirostris* | NHMUK PV OR 33095 | StGr | 0.089 | Nikon XT H 225S CTsystem, Natural History Museum, London |
| *Steneosaurus bollensis* | BSPG 1984 I258 | StBo1 | 0.043 | Nanotom Scan, Zoologische Staatsammlung München |
| *Steneosaurus bollensis* | MCZ 1063 | StBo2 | 0.404297 | micro CT scanner at the American Museum of Natural History |
| *Steneosaurus pictaviensis* | LPP.M.35 | StPi | 0.140036 | RX-solutions EasyTom XL Duo, Plateforme de Microtomographie, University of Poitiers |
| *Pelagosaurus typus* | NHMUK PV OR 32599 | PtTy | 0.098627983 | Nikon XT H 225S CTsystem, Natural History Museum, London |
| *Metriorhynchus superciliosus* | MNHN.F RJN 256 | MeSu1 | 0.10358673X 0.265 | Muséum national d'Histoire naturelle, Paris, France |
| *Metriorhynchus superciliosus* | NHMUK PV R11999 | MeSu2 | 0.12 | µ-VIS X-Ray Imaging Centre, University of Southampton |
| *Metriorhynchus superciliosus* | AMNH 997 | MeSu3 | 0.14177665 | micro CT scanner at the American Museum of Natural History |
| *Cricosaurus araucanensis* | MLP 72-IV-7-1 | CrAu1 | 0.448X0.448 | SNSB X-ray facility |
| *Cricosaurus araucanensis* | MLP 76-XI-19-1 | CrAu2 | 0.39 | SNSB X-ray facility |
| *Cricosaurus schroederi* | MMGLV # | CrSc | 0.5 | Leibniz Institute for Zoo and Wildlife Research, Berlin |
| *'Metriorhynchus' brachyrhynchus* | NHMUK PV OR 32618 | MeBr | 0.0546 | µ-VIS X-Ray Imaging Centre, University of Southampton |
| *Torvoneustes coryphaeus* | MJML K1863 | ToCo | 0.2267 | µ-VIS X-Ray Imaging Centre, University of Southampton |
| *Shamosuchus djadochtaensis* | IGM 100-1195 | ShDj | 0.011260684 | micro CT scanner at the American Museum of Natural History |
| *Alligator mississippiensis* | USNM 211232 | AlMi4 | 0.625 | Ohio Health O'Bleness Hospital |
| *Alligator mississippiensis* | USNM 211233 | AlMi5 | 0.625 | Ohio Health O'Bleness Hospital |
| *Alligator mississippiensis* | OUVC 9761 | AlMi6 | 0.5X1 | Ohio Health O'Bleness Hospital |
| *Caiman crocodilus* | FMNH 73711 | CaCr | 0.065X0.142 | University of Texas, Austin |
| *Crocodylus acutus* | FMNH 59071 | CrAc | 0.625 | Ohio Health O'Bleness Hospital |
| *Crocodylus johnstoni* | TMM M-6807 | CrJo | 0.223 | University of Texas High-Resolution X-ray CT Facility |
| *Crocodylus moreletii* | TMM M-4980 | CrMo | 0.1904X0.5 | High-Resolution X-ray CT Facility, University of Texas |
| *Crocodylus rhombifer* | MNB AB50.0171 | CrRh | 0.1748X0.5 | High-Resolution X-ray CT Facility, University of Texas |
| *Mecistops cataphractus* | TMM M-3529 | CrCa | 0.165X0.5 | High-Resolution X-ray CT Facility, University of Texas |
| *Gavialis gangeticus* | UF-herp-118998 | GaGa2 | 0.14654672 | Florida Museum of Natural History Herpetology |
| *Gavialis gangeticus* | TMM M-5490 | GaGa1 | 0.228 | High-Resolution X-ray CT Facility, University of Texas |
| *Osteolaemus tetraspis* | FMNH 98936 | OsTe | 0.0546875X0 .1108 | High-Resolution X-ray CT Facility, University of Texas |
| *Tomistoma schlegelii* | TMM M-6342 | ToSc1 | 0.165X0.46 | High-Resolution X-ray CT Facility, University of Texas |
| *Tomistoma schlegelii* | USNM 211322 | ToSc2 | 0.625 | Ohio Health O'Bleness Hospital |

**Table S2.** Information of the habitat (ecomorphology) and age of each species used in our sample.

| Taxa | habitat | Age | Reason | Reference |
|---|---|---|---|---|
| *Junggarsuchus sloani* | terrestrial | M. Jurassic | Inferred, from deposit, and limb-dimensions and cranial shape | 1 |
| Undescribed sphenosuchian | terrestrial | Carnian | Inferred, from deposit, and limb-dimensions and cranial shape | NCSM 21722 |
| *Eopneumatosuchus colberti* | semiaquatic | Sinemurian* | Inferred, from deposit and cranial shape | 2 |
| *Protosuchus haughtoni* | terrestrial | Hettangian | Inferred, from post-cranial skeleton | 3 |
| *'Steneosaurus' gracilirostris* | semiaquatic | Toarcian | Inferred, from a marine deposit, but has extant-like limbs, and has osteoderms | 4 |
| *Steneosaurus bollensis* | semiaquatic | Toarcian | Inferred, from a marine deposit, but has extant-like limbs, and has osteoderms | 4 |
| *Steneosaurus pictaviensis* | semiaquatic | Toarcian | Inferred, from a marine deposit and is a teleosaurid | 5 |
| *Pelagosaurus typus* | semiaquatic | Toarcian | Inferred, from a marine deposit, but has extant-like limbs, and has osteoderms | 4 |
| *Metriorhynchus superciliosus* | pelagic | Callovian | Inferred, marine deposit, has flippers and a tail-fin | 5 |
| *Cricosaurus araucanensis* | pelagic | Tithonian | Inferred, marine deposit, has flippers and a tail-fin | 6, 7 |
| *Cricosaurus schroederi* | pelagic | Valanginian | Inferred, marine deposit and is a metriorhynchid | 8 |
| *'Metriorhynchus' brachyrhynchus* | pelagic | Callovian | Inferred, marine deposit and has a tail-fin | 5 |
| *Torvoneustes coryphaeus* | pelagic | Kimmeridgian | Inferred, marine deposit and is a metriorhynchid | 9 |
| *Shamosuchus djadochtaensis* | semiaquatic | L. Cretaceous | Inferred, based on post-cranial anatomy | 10 |
| *Alligator mississippiensis* | semiaquatic | Recent | extant, observed | e.g. 11 |
| *Caiman crocodilus* | semiaquatic | Recent | extant, observed | e.g. 11 |
| *Crocodylus acutus* | semiaquatic | Recent | extant, observed | e.g. 11 |
| *Crocodylus johnstoni* | semiaquatic | Recent | extant, observed | e.g. 11 |
| *Crocodylus moreletii* | semiaquatic | Recent | extant, observed | e.g. 11 |
| *Crocodylus rhombifer* | semiaquatic | Recent | extant, observed | e.g. 11 |
| *Mecistops cataphractus* | semiaquatic | Recent | extant, observed | e.g. 11 |
| *Gavialis gangeticus* | semiaquatic | Recent | extant, observed | e.g. 11 |
| *Osteolaemus tetraspis* | semiaquatic | Recent | extant, observed | e.g. 11 |
| *Tomistoma schlegelii* | semiaquatic | Recent | extant, observed | e.g. 11 |

*The age of the Kayenta Formation may be Pliensbachian-Toarcian, as has been presented in a conference abstract (Marsh et al., 2014, Society of Vertebrate Paleontology Annual Meeting).

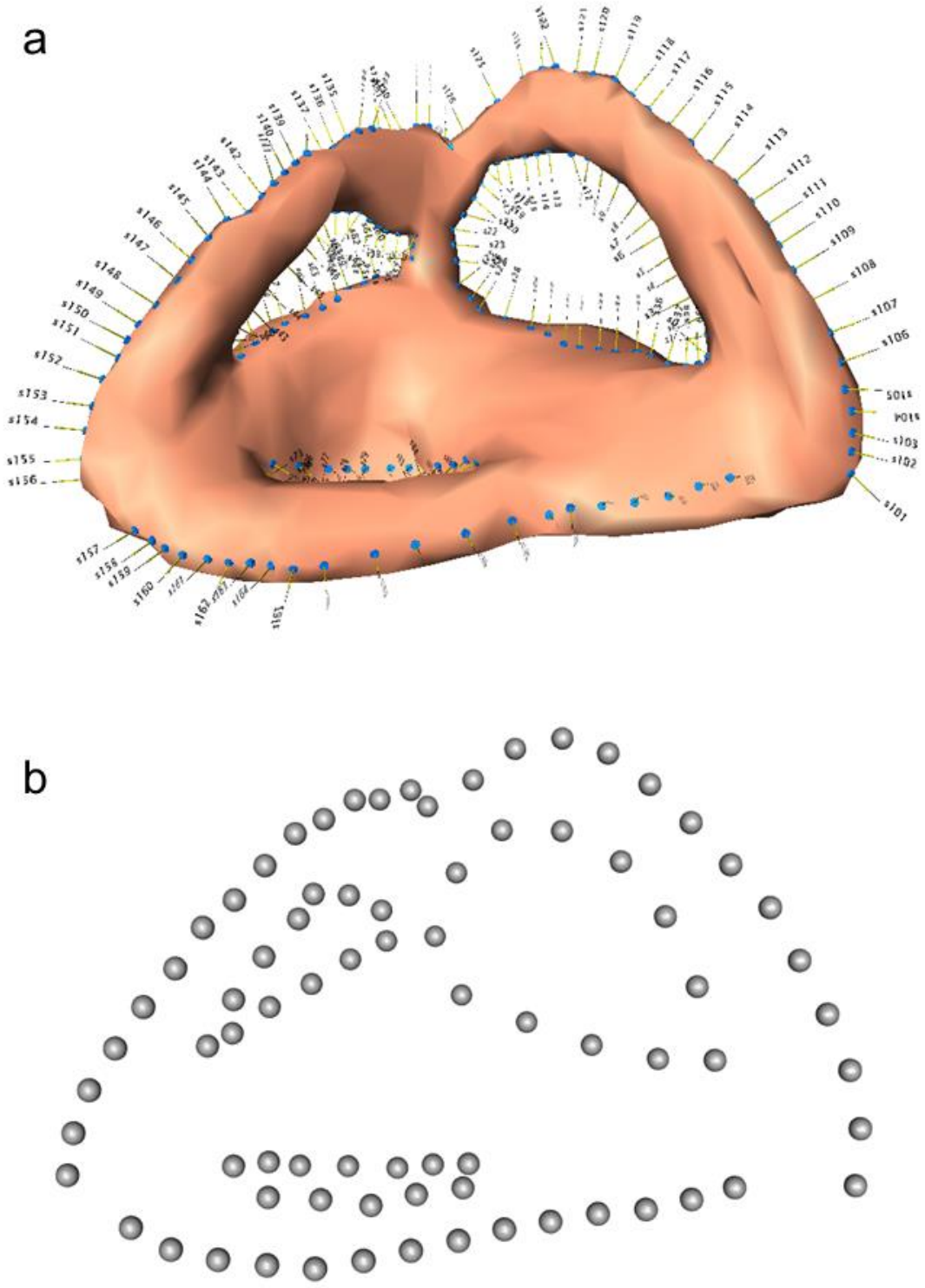


**Fig. S1.** Landmark placing on the right labyrinth of *Metriorhynchus supercilious* (NHMUK PV R11999). a, landmark placement in the IDAV Landmark software; b, evenly spaced semilandmarks on the three semicircular canals, 11 on the internal surface and 12 on the external surface (see methods section for details).

## 3. Principal component analysis

**Table S3**. Results of the Principal Component Analysis. PCA coordinates for the first 31 PC axes.

| | PC1 | PC2 | PC3 | PC4 | PC5 | PC6 | PC7 | PC8 |
|---|---|---|---|---|---|---|---|---|
| **AlMi4** | -0.025 | -0.024 | 0.035 | -0.038 | 0.013 | -0.002 | 0.009 | 0.000 |
| **AlMi5** | -0.022 | -0.050 | 0.025 | -0.044 | 0.000 | -0.007 | 0.010 | -0.003 |
| **CaCr** | -0.051 | -0.043 | -0.011 | -0.037 | -0.025 | -0.001 | 0.010 | 0.028 |
| **CrAc** | -0.016 | -0.056 | 0.015 | 0.025 | 0.022 | -0.030 | -0.020 | -0.006 |
| **CrMo** | -0.061 | -0.021 | -0.019 | 0.013 | 0.011 | 0.012 | -0.014 | -0.004 |
| **CrJo** | -0.059 | -0.003 | -0.004 | -0.059 | 0.012 | 0.000 | 0.012 | -0.028 |
| **CrCa** | -0.014 | -0.085 | 0.022 | 0.047 | 0.011 | -0.023 | 0.005 | -0.004 |
| **OsTe** | -0.030 | -0.002 | 0.049 | -0.003 | -0.035 | -0.044 | -0.012 | 0.034 |
| **GaGa1** | -0.028 | -0.056 | 0.054 | -0.006 | 0.004 | -0.008 | 0.005 | 0.004 |
| **ToSc1** | -0.051 | -0.069 | 0.013 | 0.027 | 0.013 | 0.014 | -0.007 | 0.014 |
| **ToSc2** | -0.022 | -0.071 | 0.035 | 0.025 | 0.009 | 0.027 | -0.017 | 0.021 |
| **GaGa2** | -0.032 | -0.010 | 0.058 | -0.023 | 0.037 | 0.028 | -0.019 | 0.005 |
| **AlMi6** | -0.038 | 0.013 | 0.028 | -0.045 | 0.001 | -0.011 | 0.042 | -0.030 |
| **CrRh** | -0.033 | -0.053 | 0.002 | 0.039 | 0.001 | 0.036 | 0.001 | -0.005 |
| **PeTy** | 0.014 | 0.084 | 0.028 | 0.006 | -0.043 | 0.010 | -0.016 | -0.002 |
| **JuSl** | -0.115 | 0.019 | -0.064 | 0.031 | -0.033 | -0.056 | 0.012 | 0.002 |
| **MeSu2** | 0.057 | 0.015 | -0.016 | -0.041 | 0.038 | 0.003 | 0.048 | 0.032 |
| **StBo1** | 0.011 | 0.056 | 0.058 | 0.023 | -0.011 | 0.013 | -0.017 | 0.013 |
| **CrSc** | 0.104 | -0.092 | -0.062 | -0.005 | -0.077 | 0.060 | -0.011 | -0.047 |
| **EoCo** | -0.048 | 0.066 | -0.030 | 0.009 | 0.014 | 0.046 | -0.020 | -0.021 |
| **UnSp** | -0.087 | 0.039 | -0.065 | -0.008 | -0.081 | -0.015 | 0.016 | 0.012 |
| **MeSu1** | 0.038 | 0.064 | -0.037 | -0.004 | 0.001 | 0.031 | 0.031 | 0.033 |
| **StBo2** | 0.014 | 0.097 | 0.059 | 0.018 | -0.012 | -0.024 | 0.006 | -0.056 |
| **StGr** | 0.059 | 0.066 | 0.029 | 0.051 | -0.018 | 0.001 | 0.005 | 0.001 |
| **MeBr** | 0.072 | 0.063 | -0.009 | 0.000 | 0.040 | -0.006 | 0.049 | 0.005 |
| **MeSu3** | 0.028 | 0.039 | -0.022 | 0.005 | -0.004 | 0.041 | 0.029 | 0.031 |
| **CrAu1** | 0.136 | 0.008 | 0.021 | -0.074 | -0.026 | -0.023 | -0.073 | 0.037 |
| **PrHa** | -0.071 | 0.101 | -0.096 | -0.005 | 0.060 | -0.002 | -0.071 | -0.005 |
| **ToCo** | 0.115 | -0.065 | -0.110 | 0.057 | 0.025 | -0.042 | 0.005 | 0.017 |
| **CrAu2** | 0.087 | -0.028 | -0.032 | -0.047 | 0.019 | -0.044 | -0.003 | -0.052 |
| **StPi** | 0.073 | 0.031 | 0.068 | 0.069 | 0.005 | -0.011 | 0.002 | -0.013 |
| **ShDj** | -0.003 | -0.035 | -0.025 | -0.007 | 0.027 | 0.025 | 0.002 | -0.016 |

| | PC9 | PC10 | PC11 | PC12 | PC13 | PC14 | PC15 | PC16 |
|---|---|---|---|---|---|---|---|---|
| **AlMi4** | 0.028 | -0.006 | -0.019 | 0.014 | -0.035 | -0.013 | -0.002 | 0.039 |
| **AlMi5** | 0.016 | -0.002 | 0.026 | -0.018 | -0.009 | -0.018 | 0.008 | 0.008 |
| **CaCr** | 0.008 | -0.005 | -0.012 | -0.020 | 0.014 | 0.003 | -0.024 | 0.008 |
| **CrAc** | 0.042 | -0.010 | 0.014 | -0.023 | 0.040 | 0.005 | 0.015 | 0.002 |
| **CrMo** | -0.023 | -0.018 | -0.003 | -0.014 | 0.011 | 0.015 | 0.006 | 0.005 |
| **CrJo** | -0.030 | -0.022 | -0.008 | 0.022 | -0.004 | 0.008 | 0.026 | -0.013 |
| **CrCa** | -0.032 | -0.010 | 0.024 | 0.005 | 0.012 | -0.010 | 0.023 | 0.001 |
| **OsTe** | 0.012 | -0.040 | 0.003 | -0.001 | -0.022 | 0.034 | -0.015 | -0.012 |
| **GaGa1** | 0.014 | 0.018 | 0.010 | 0.004 | -0.002 | 0.007 | -0.001 | 0.006 |
| **ToSc1** | -0.013 | 0.017 | 0.005 | 0.006 | 0.010 | -0.017 | -0.003 | -0.005 |
| **ToSc2** | 0.032 | 0.013 | 0.006 | 0.024 | -0.020 | -0.036 | -0.005 | -0.026 |
| **GaGa2** | 0.008 | 0.028 | -0.012 | -0.011 | 0.014 | 0.026 | -0.015 | -0.013 |
| **AlMi6** | -0.002 | -0.034 | -0.017 | -0.022 | 0.009 | -0.024 | -0.022 | -0.017 |
| **CrRh** | -0.025 | -0.015 | -0.004 | 0.017 | -0.006 | 0.018 | 0.004 | 0.024 |
| **PeTy** | -0.017 | -0.014 | 0.002 | -0.011 | 0.007 | -0.022 | -0.013 | 0.015 |
| **JuSl** | 0.005 | 0.045 | -0.053 | -0.014 | -0.010 | -0.003 | 0.027 | -0.004 |
| **MeSu2** | -0.023 | 0.009 | 0.024 | -0.006 | -0.015 | 0.008 | 0.026 | 0.009 |
| **StBo1** | -0.016 | 0.021 | 0.007 | -0.017 | -0.030 | 0.015 | 0.001 | -0.004 |
| **CrSc** | 0.036 | -0.009 | -0.008 | -0.010 | -0.006 | 0.013 | 0.018 | -0.003 |
| **EoCo** | -0.007 | 0.001 | 0.004 | -0.006 | -0.030 | -0.008 | -0.005 | -0.015 |
| **UnSp** | -0.007 | 0.005 | 0.041 | 0.044 | 0.013 | 0.003 | -0.012 | -0.005 |
| **MeSu1** | 0.028 | 0.012 | -0.013 | 0.012 | 0.026 | -0.010 | -0.006 | 0.017 |
| **StBo2** | 0.006 | 0.012 | 0.013 | -0.009 | -0.002 | 0.012 | -0.003 | 0.008 |
| **StGr** | -0.022 | -0.011 | 0.002 | -0.022 | 0.005 | -0.032 | 0.012 | -0.002 |
| **MeBr** | 0.033 | -0.024 | -0.013 | 0.022 | 0.002 | 0.006 | 0.016 | -0.021 |
| **MeSu3** | -0.001 | 0.020 | 0.018 | -0.025 | 0.011 | 0.017 | 0.000 | -0.007 |
| **CrAu1** | -0.025 | 0.002 | -0.021 | 0.011 | 0.012 | -0.008 | 0.017 | -0.005 |
| **PrHa** | 0.027 | -0.018 | 0.015 | 0.004 | 0.003 | -0.002 | 0.003 | 0.008 |
| **ToCo** | -0.010 | -0.016 | -0.002 | -0.015 | -0.025 | 0.001 | -0.028 | -0.001 |
| **CrAu2** | -0.005 | 0.045 | 0.023 | 0.009 | 0.000 | -0.001 | -0.020 | 0.000 |
| **StPi** | 0.011 | 0.001 | -0.020 | 0.040 | 0.012 | 0.011 | -0.006 | 0.005 |
| **ShDj** | -0.048 | 0.004 | -0.031 | 0.011 | 0.016 | 0.002 | -0.023 | 0.000 |

| | PC17 | PC18 | PC19 | PC20 | PC21 | PC22 | PC23 | PC24 |
|---|---|---|---|---|---|---|---|---|
| **AlMi4** | -0.013 | 0.000 | -0.005 | -0.001 | -0.005 | 0.018 | 0.002 | 0.002 |
| **AlMi5** | -0.012 | 0.000 | 0.018 | 0.009 | -0.003 | -0.006 | -0.015 | -0.015 |
| **CaCr** | -0.011 | -0.008 | 0.008 | 0.001 | 0.033 | -0.004 | 0.002 | 0.011 |
| **CrAc** | -0.007 | 0.007 | 0.006 | -0.007 | -0.002 | 0.007 | -0.009 | 0.013 |
| **CrMo** | -0.011 | 0.010 | 0.004 | -0.004 | 0.004 | 0.001 | 0.009 | -0.019 |
| **CrJo** | -0.004 | -0.002 | 0.016 | 0.011 | 0.001 | -0.011 | 0.011 | 0.017 |
| **CrCa** | 0.012 | -0.011 | -0.003 | -0.002 | 0.003 | 0.015 | 0.011 | 0.000 |
| **OsTe** | 0.027 | 0.014 | -0.008 | -0.008 | -0.002 | -0.001 | -0.005 | 0.001 |
| **GaGa1** | 0.012 | -0.003 | 0.002 | 0.004 | -0.002 | -0.015 | -0.002 | -0.009 |
| **ToSc1** | -0.007 | 0.001 | -0.023 | -0.023 | 0.005 | -0.008 | 0.000 | 0.002 |
| **ToSc2** | -0.001 | 0.006 | 0.004 | 0.004 | -0.008 | -0.009 | 0.005 | 0.007 |
| **GaGa2** | 0.005 | -0.029 | -0.014 | 0.022 | -0.003 | 0.005 | 0.003 | -0.006 |
| **AlMi6** | 0.008 | 0.003 | -0.004 | -0.003 | -0.014 | 0.012 | 0.010 | -0.004 |
| **CrRh** | 0.014 | 0.004 | 0.011 | 0.001 | -0.003 | -0.013 | 0.000 | -0.007 |
| **PeTy** | 0.006 | 0.002 | -0.009 | 0.013 | -0.002 | -0.014 | -0.006 | 0.010 |
| **JuSl** | 0.007 | 0.002 | 0.000 | 0.004 | -0.004 | -0.001 | -0.004 | -0.001 |
| **MeSu2** | 0.011 | -0.007 | -0.020 | -0.001 | 0.000 | 0.003 | -0.009 | 0.010 |
| **StBo1** | -0.026 | 0.021 | -0.006 | 0.000 | 0.006 | 0.006 | 0.016 | 0.002 |
| **CrSc** | 0.002 | -0.001 | -0.015 | 0.002 | 0.000 | 0.002 | 0.001 | 0.001 |
| **EoCo** | 0.017 | -0.015 | 0.019 | -0.018 | 0.015 | 0.013 | -0.013 | -0.001 |
| **UnSp** | -0.015 | -0.009 | -0.005 | 0.005 | -0.004 | 0.010 | -0.003 | -0.005 |
| **MeSu1** | 0.021 | 0.000 | 0.007 | -0.012 | -0.002 | -0.003 | 0.017 | -0.003 |
| **StBo2** | -0.012 | -0.021 | 0.001 | -0.021 | -0.010 | -0.015 | 0.003 | 0.003 |
| **StGr** | 0.006 | 0.002 | -0.006 | 0.016 | 0.011 | 0.001 | -0.003 | -0.007 |
| **MeBr** | -0.017 | 0.004 | -0.009 | -0.003 | 0.013 | -0.010 | -0.005 | -0.012 |
| **MeSu3** | -0.004 | 0.014 | 0.022 | 0.002 | -0.017 | 0.006 | -0.002 | 0.006 |
| **CrAu1** | -0.004 | -0.009 | 0.009 | -0.011 | -0.006 | 0.002 | 0.000 | -0.006 |
| **PrHa** | 0.002 | 0.006 | -0.011 | 0.009 | -0.003 | -0.002 | 0.003 | 0.001 |
| **ToCo** | -0.011 | -0.018 | 0.007 | 0.005 | -0.008 | -0.005 | 0.005 | 0.002 |
| **CrAu2** | 0.017 | 0.023 | 0.001 | 0.003 | 0.013 | 0.001 | 0.005 | -0.003 |
| **StPi** | 0.000 | 0.001 | 0.013 | 0.011 | 0.005 | 0.014 | -0.007 | 0.006 |
| **ShDj** | -0.011 | 0.014 | -0.009 | -0.005 | -0.010 | 0.000 | -0.019 | 0.003 |

| | PC25 | PC26 | PC27 | PC28 | PC29 | PC30 | PC31 |
|---|---|---|---|---|---|---|---|
| **AlMi4** | -0.001 | -0.002 | -0.014 | 0.005 | 0.000 | 0.002 | 0.001 |
| **AlMi5** | 0.001 | -0.003 | 0.010 | -0.007 | 0.001 | -0.010 | 0.008 |
| **CaCr** | 0.010 | -0.001 | 0.002 | 0.001 | -0.004 | -0.003 | -0.006 |
| **CrAc** | -0.010 | -0.004 | 0.000 | 0.001 | 0.010 | 0.008 | -0.001 |
| **CrMo** | -0.015 | -0.005 | -0.005 | -0.008 | -0.015 | 0.005 | -0.002 |
| **CrJo** | -0.004 | -0.004 | -0.002 | 0.005 | 0.000 | 0.002 | 0.008 |
| **CrCa** | 0.018 | 0.006 | -0.007 | -0.010 | 0.002 | -0.004 | 0.001 |
| **OsTe** | 0.002 | -0.008 | -0.004 | -0.001 | -0.001 | -0.004 | 0.005 |
| **GaGa1** | 0.010 | 0.015 | 0.003 | 0.007 | -0.006 | 0.018 | 0.003 |
| **ToSc1** | -0.010 | 0.007 | -0.001 | 0.011 | -0.003 | -0.010 | 0.008 |
| **ToSc2** | 0.000 | -0.010 | -0.001 | -0.007 | -0.004 | 0.001 | -0.009 |
| **GaGa2** | -0.005 | -0.005 | -0.005 | -0.001 | 0.005 | -0.003 | 0.001 |
| **AlMi6** | -0.002 | 0.009 | 0.011 | 0.004 | 0.000 | -0.001 | -0.005 |
| **CrRh** | -0.004 | 0.000 | 0.004 | 0.006 | 0.013 | -0.006 | -0.011 |
| **PeTy** | -0.010 | 0.015 | -0.009 | -0.012 | 0.002 | 0.001 | 0.001 |
| **JuSl** | 0.000 | 0.002 | 0.001 | -0.002 | 0.001 | -0.002 | -0.002 |
| **MeSu2** | -0.007 | -0.003 | 0.010 | -0.003 | -0.006 | 0.002 | -0.006 |
| **StBo1** | 0.002 | 0.004 | 0.012 | -0.003 | 0.009 | 0.004 | 0.003 |
| **CrSc** | 0.003 | 0.001 | 0.003 | 0.000 | -0.003 | -0.001 | 0.002 |
| **EoCo** | -0.004 | 0.004 | -0.002 | -0.001 | 0.003 | 0.005 | 0.002 |
| **UnSp** | -0.003 | -0.002 | 0.001 | 0.002 | 0.003 | 0.004 | -0.001 |
| **MeSu1** | 0.000 | -0.009 | 0.005 | -0.006 | 0.004 | 0.002 | 0.008 |
| **StBo2** | 0.006 | -0.009 | -0.001 | -0.001 | -0.004 | -0.002 | -0.004 |
| **StGr** | 0.004 | -0.017 | -0.003 | 0.014 | -0.001 | 0.003 | 0.001 |
| **MeBr** | 0.003 | 0.008 | -0.009 | -0.003 | 0.007 | -0.001 | -0.003 |
| **MeSu3** | 0.006 | 0.007 | -0.013 | 0.007 | -0.006 | -0.006 | -0.001 |
| **CrAu1** | 0.000 | 0.003 | 0.001 | 0.002 | 0.001 | 0.000 | -0.004 |
| **PrHa** | 0.011 | 0.003 | 0.006 | 0.003 | -0.004 | -0.004 | -0.001 |
| **ToCo** | -0.005 | 0.002 | 0.001 | 0.001 | 0.001 | 0.002 | 0.003 |
| **CrAu2** | -0.005 | -0.002 | -0.006 | 0.000 | 0.002 | -0.003 | -0.002 |
| **StPi** | -0.005 | 0.006 | 0.011 | 0.000 | -0.011 | -0.005 | 0.002 |
| **ShDj** | 0.014 | -0.009 | 0.001 | -0.006 | 0.002 | 0.005 | 0.003 |

**Table S4.** Results of the Principal Component Analysis. Variance (%) and Cumulative Proportion (%) for the first 31 principal component axes.

| | Variance (%) | Cumulative Proportion (%) |
|---|---|---|
| **PC1** | 22.269 | 22.269 |
| **PC2** | 18.443 | 40.713 |
| **PC3** | 12.386 | 53.099 |
| **PC4** | 7.336 | 60.435 |
| **PC5** | 5.641 | 66.076 |
| **PC6** | 4.605 | 70.681 |
| **PC7** | 4.183 | 74.864 |
| **PC8** | 3.487 | 78.351 |
| **PC9** | 3.100 | 81.450 |
| **PC10** | 2.368 | 83.819 |
| **PC11** | 2.124 | 85.943 |
| **PC12** | 1.951 | 87.894 |
| **PC13** | 1.702 | 89.596 |
| **PC14** | 1.525 | 91.121 |
| **PC15** | 1.454 | 92.575 |
| **PC16** | 1.006 | 93.581 |
| **PC17** | 0.918 | 94.498 |
| **PC18** | 0.769 | 95.267 |
| **PC19** | 0.748 | 96.015 |
| **PC20** | 0.597 | 96.612 |
| **PC21** | 0.540 | 97.152 |
| **PC22** | 0.483 | 97.635 |
| **PC23** | 0.409 | 98.044 |
| **PC24** | 0.374 | 98.418 |
| **PC25** | 0.325 | 98.743 |
| **PC26** | 0.309 | 99.053 |
| **PC27** | 0.262 | 99.315 |
| **PC28** | 0.197 | 99.511 |
| **PC29** | 0.196 | 99.707 |
| **PC30** | 0.167 | 99.874 |
| **PC31** | 0.126 | 100.000 |

## 4. Morphospace clustering analysis

**Table S5.** Results of the PERMANOVA, to test if the three habitat groups are statistically significantly different form each other.

| pairs | F Model | R2 | p value | p adjusted |
|---|---|---|---|---|
| **semiaquatic vs. terrestrial** | 4.875 | 0.223 | 0.002 | 0.003 |
| **semiaquatic vs. pelagic** | 5.302 | 0.218 | 0.002 | 0.003 |
| **terrestrial vs. pelagic** | 4.543 | 0.431 | 0.012 | 0.012 |

## 5. Canonical variate analysis

**Table S6.** Results for the canonical variate analysis (CVA). Showing the classification of the three habitat groups (pelagic, semiaquatic, terrestrial) with an overall classification accuracy of 100%.

| | pelagic | semiaquatic | terrestrial |
|---|---|---|---|
| **pelagic** | 100 | 0 | 0 |
| **semiaquatic** | 0 | 100 | 0 |
| **terrestrial** | 0 | 0 | 100 |

overall classification accuracy: 100 %

| | CV 1 | CV 2 |
|---|---|---|
| **AlMi4** | -1.033 | 0.846 |
| **AlMi5** | -0.485 | 1.594 |
| **CaCr** | -0.128 | -0.364 |
| **CrAc** | -2.027 | 0.536 |
| **CrMo** | -3.402 | 0.029 |
| **CrJo** | -2.502 | -0.035 |
| **CrCa** | -3.322 | 1.787 |
| **OsTe** | -3.384 | -0.204 |
| **GaGa1** | -2.031 | 1.215 |
| **ToSc1** | -2.747 | 0.397 |
| **ToSc2** | -1.644 | 0.679 |
| **GaGa2** | -2.243 | 2.108 |
| **AlMi6** | -2.406 | 2.322 |
| **CrRh** | -3.277 | 1.411 |
| **PeTy** | -1.567 | 0.197 |
| **JuSl** | -1.680 | -7.193 |
| **MeSu2** | 5.803 | 1.926 |
| **StBo1** | -1.803 | 1.280 |
| **CrSc** | 5.133 | 1.732 |
| **EoCo** | -1.782 | -1.412 |
| **UnSp** | 0.071 | -7.272 |
| **MeSu1** | 5.550 | -1.380 |
| **StBo2** | -2.583 | 0.189 |
| **StGr** | -0.300 | 2.021 |
| **MeBr** | 4.587 | 0.826 |
| **MeSu3** | 4.047 | 0.695 |
| **CrAu1** | 4.832 | 0.948 |
| **PrHa** | -0.600 | -6.291 |
| **ToCo** | 6.925 | -0.480 |
| **CrAu2** | 5.415 | -0.885 |
| **StPi** | -1.109 | 1.514 |
| **ShDj** | -0.307 | 1.266 |

## 6. Phylogenies used for phylogenetic comparative methods

The main phylogenetic framework used herein is based on the results from Young *et al*. (12). This dataset (the 'H+Y dataset') is the latest in the ongoing Crocodylomorph SuperMatrix Project, a continuously updated dataset investigating the evolutionary relationships of crocodylomorph archosaurs. It was first presented in Ristevski *et al*. (13), and has been subsequently updated (e.g. 14–17). It is one of three datasets that form the core of the Crocodylomorph SuperMatrix Project, the other two also being presented in a modified form in Ősi *et al*. (14).

However, there are some taxa we use in our datasets that are known to have differing positions phylogenetically. The first of which is *Eopneumatosuchus colberti*. It has been recovered as the basal-most thalattosuchian in the 'H+Y dataset'. However, in Young *et al*. (12), the position of *Eopneumatosuchus* can change depending on use of implied weighting or using Bayesian methods. In those analyses, *Eopneumatosuchus* is recovered as the sister taxon to Shartegosuchoidea + Mesoeucrocodylia. To test whether this second possible position of *Eopneumatosuchus* alters our result, we ran a series of sensitivity analyses with *Eopneumatosuchus* placed as the sister taxon to Thalattosuchia + (*Shamosuchus* + Crocodylia).

The second species we ran sensitivity analyses on was *Pelagosaurus typus*. While the more recent and large-sampled thalattosuchians phylogenetic datasets recover *Pelagosaurus* as the basal-most member of Metriorhynchoidea (papers using the 'H+Y' dataset, 18), some earlier datasets and pre-phylogenetic opinions considered *Pelagosaurus* to be a teleosauroid (e.g. 4, 19; although see Buffetaut (20) for a metriorhynchid-like opinion). We tested this alternate position of *Pelagosaurus* to see if it impacted upon our results.

There are also some competing hypotheses for the relationships of extant crocodylians in our dataset. In particular, there is no consensus on whether *Osteolaemus tetraspis* is more closely related to *Mecistops* or *Crocodylus*, in either molecular or morphological phylogenies (21). Additionally, the position of *Gavialis gangeticus* differs between molecular and morphological datasets. Molecular datasets recover *Gavialis* as the sister taxon to *Tomistoma* (being within Crocodylidae) – a position the Young *et al*. (12) dataset also recovers (e.g. 21, 22). However, most morphology-only datasets recover *Gavialis* as the basal-most living species, being the sister taxon to Alligatoridae + Crocodylidae (for further analyses and discussion see 23). However, as these both concern small nuances of the relationships of extant crocodylians—all of which have semiaquatic-type ears—these rearrangements would not affect our results.

## 7. Pagel's Lambda analysis

**Table S7.** Results for the phylogenetic influence tested with the Pagel's lambda tested for three different phylogenies: our primary phylogeny (first listed) and two alternative trees, for sensitivity analysis (see Section 6 above). 0 → no correlation between species; 1 → correlation between species equal to the Brownian expectation/the structure of the phylogeny alone can explain changes in traits.

**Primary phylogeny**

| | lambda | logL | logL0 | p value |
|---|---|---|---|---|
| PC1 | 0.99996 | 28.705 | 16.435 | 0.00000073 |
| PC2 | 0.69646 | 31.134 | 22.893 | 0.00004913 |
| PC3 | 0.99993 | 31.597 | 18.921 | 0.00000048 |

***Eopneumatosuchus colberti* placed as the sister taxon to Thalattosuchia + (*Shamosuchus* + Crocodylia)**

| | lambda | logL | logL0 | p value |
|---|---|---|---|---|
| PC1 | 0.77400 | 27.769 | 16.506 | 2E-06 |
| PC2 | 0.65831 | 30.953 | 22.949 | 6E-05 |
| PC3 | 0.99993 | 32.243 | 19.051 | 3E-07 |

***Pelagosaurus typus* positioned as a teleosauroid**

| | lambda | logL | logL0 | p value |
|---|---|---|---|---|
| PC1 | 0.77400 | 27.769 | 16.506 | 2E-06 |
| PC2 | 0.65831 | 30.953 | 22.949 | 6E-05 |
| PC3 | 0.99993 | 32.243 | 19.051 | 3E-07 |

## 8. pGLS regressions

**Table S8**. Results for Ordinary least squares (OLS) and phylogenetic generalised least squares (pGLS), using our primary phylogeny. First correlating the raw PC scores and centroid size (labyrinth size); second, correlating the raw PC scores and habitat; third correlating the residuals from the PC scores and centroid size with habitat.

**Primary phylogeny**

| Model | Type | AICc | intercept | p value | slope | p value | R2 |
|---|---|---|---|---|---|---|---|
| PC1~centroid size | OLS | -61.319 | -4.706 | 0.111 | 4.662 | 0.112 | 0.071 |
| | pGLS | -78.643 | -5.078 | 0.034 | 4.993 | 0.035 | 0.111 |
| PC2~centroid size | OLS | -64.049 | -0.531 | 0.845 | 0.527 | 0.845 | -0.044 |
| | pGLS | -76.99 | 8.307 | 0.002 | -8.208 | 0.002 | 0.418 |
| PC3~centroid size | OLS | -88.324 | 7.205 | 0.0002 | -7.149 | 0.0002 | 0.451 |
| | pGLS | -81.948 | 5.787 | 0.011 | -5.751 | 0.011 | 0.315 |
| PC1~pelagic | OLS | -78.162 | -0.028 | 0.012 | 0.116 | 2.65e-05 | 0.559 |
| | pGLS | -70.159 | -0.035 | 0.370 | 0.083 | 0.042 | 0.385 |
| PC2~pelagic | OLS | -64.329 | 0.0033 | 0.81 | -0.016 | 0.59 | 0.013 |
| | pGLS | -60.347 | 0.002 | 0.974 | -0.060 | 0.222 | -0.165 |
| PC3~pelagic | OLS | -76.934 | 0.0035 | 0.734 | -0.046 | 0.056 | 0.156 |
| | pGLS | -68.628 | -0.031 | 0.445 | -0.050 | 0.226 | -0.193 |
| PC1.residuals~pelagic | OLS | -72.660 | -0.019 | 0.110 | 0.089 | 0.00143 | 0.377 |
| | pGLS | -59.892 | 0.018 | 0.703 | 0.089 | 0.0005 | -0.061 |
| PC2.residuals~pelagic | OLS | -64.505 | 0.004 | 0.769 | -0.019 | 0.522 | 0.019 |
| | pGLS | -49.136 | -0.038 | 0.522 | 0.007 | 0.801 | -0.861 |
| PC3.residuals~pelagic | OLS | -88.418 | 0.001 | 0.895 | -0.005 | 0.773 | 0.004 |
| | pGLS | -68.295 | 0.003 | 0.940 | 0.008 | 0.847 | -1.304 |

**Table S9**. Results for phylogenetic generalised least squares (pGLS), using the two alternative phylogenies. First correlating the raw PC scores and centroid size (labyrinth size); second, correlating the raw PC scores and habitat; third correlating the residuals from the PC scores and centroid size with habitat.

***Eopneumatosuchus colberti* placed as the sister taxon to Thalattosuchia + (*Shamosuchus* + Crocodylia)**

| Model | Type | AICc | intercept | p value | slope | p value | R2 |
|---|---|---|---|---|---|---|---|
| PC1~centroid size | pGLS | -76.721 | -4.918 | 0.069 | 4.838 | 0.069 | 0.532 |
| PC2~centroid size | pGLS | -77.183 | 7.885 | 0.005 | -7.790 | 0.005 | 0.422 |
| PC3~centroid size | pGLS | -83.430 | 5.577 | 0.019 | -5.544 | 0.019 | 0.356 |
| PC1~pelagic | pGLS | -70.159 | -0.035 | 0.370 | 0.083 | 0.042 | 0.385 |
| PC2~pelagic | pGLS | -60.347 | 0.002 | 0.974 | -0.060 | 0.222 | -0.165 |
| PC3~pelagic | pGLS | -68.628 | -0.031 | 0.445 | -0.049 | 0.226 | -0.192 |
| PC1.residuals~pelagic | pGLS | -55.657 | 0.009 | 0.859 | 0.092 | 0.001 | -0.266 |
| PC2.residuals~pelagic | pGLS | -47.624 | -0.032 | 0.594 | 0.013 | 0.666 | -0.983 |
| PC3.residuals~pelagic | pGLS | -70.355 | 0.003 | 0.939 | 0.011 | 0.544 | -1.114 |

***Pelagosaurus typus* positioned as a teleosauroid**

| Model | Type | AICc | intercept | p value | slope | p value | R2 |
|---|---|---|---|---|---|---|---|
| PC1~centroid size | pGLS | -80.371 | -5.328 | 0.023 | 5.230 | 0.024 | 0.598 |
| PC2~centroid size | pGLS | -77.218 | 8.343 | 0.002 | -8.242 | 0.002 | 0.423 |
| PC3~centroid size | pGLS | -82.687 | 5.655 | 0.012 | -5.627 | 0.012 | 0.336 |
| PC1~pelagic | pGLS | -71.177 | -0.042 | 0.279 | 0.078 | 0.041 | 0.410 |
| PC2~pelagic | pGLS | -60.562 | 0.0002 | 0.997 | -0.059 | 0.214 | -0.154 |
| PC3~pelagic | pGLS | -69.841 | -0.038 | 0.345 | -0.052 | 0.174 | -0.134 |
| PC1.residuals~pelagic | pGLS | -55.436 | 0.008 | 0.887 | 0.089 | 0.001 | -0.278 |
| PC2.residuals~pelagic | pGLS | -48.265 | -0.039 | 0.536 | 0.007 | 0.809 | -0.930 |
| PC3.residuals~pelagic | pGLS | -70.095 | 0.004 | 0.916 | 0.005 | 0.782 | -1.137 |

## 9. Labyrinth character optimization on phylogeny

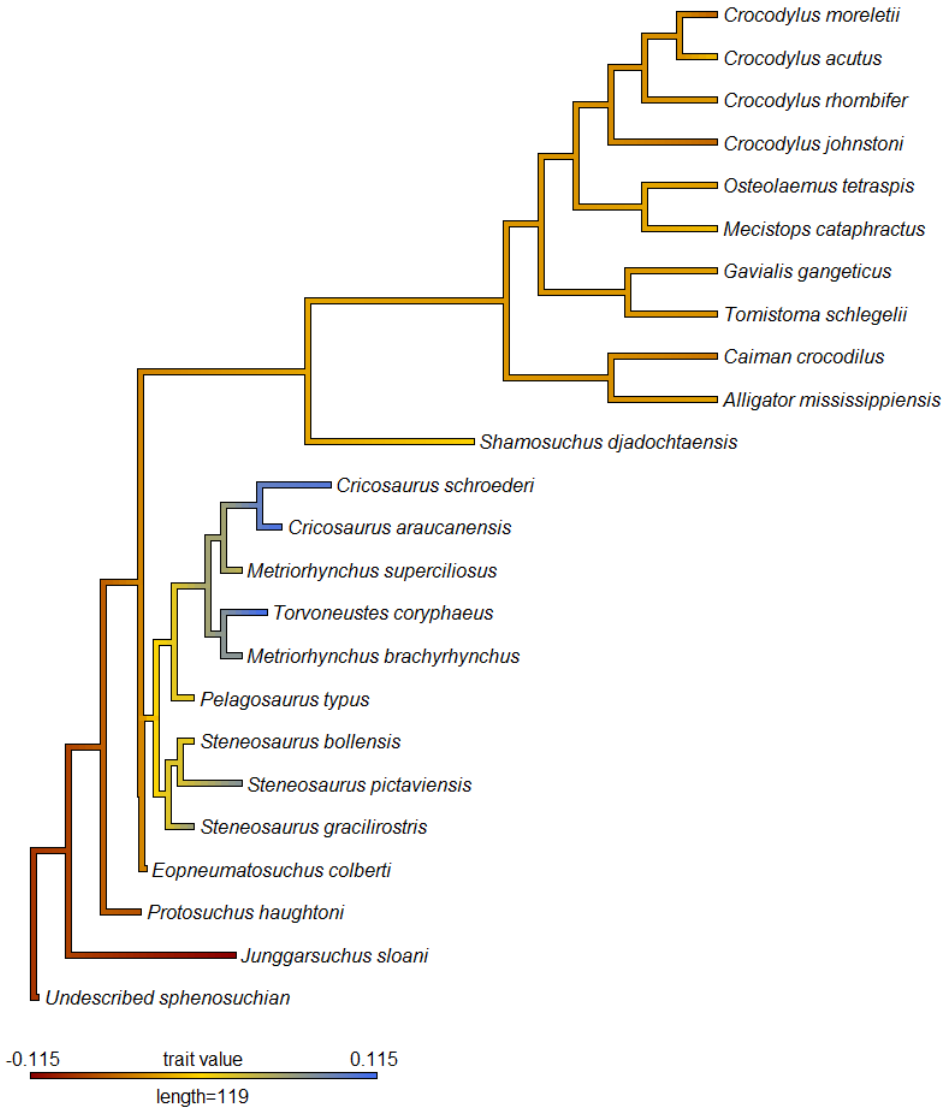


**Fig. S2.** PC1 scores optimized on our primary phylogeny to predict ancestral states for the major clades and assess evolutionary trends.

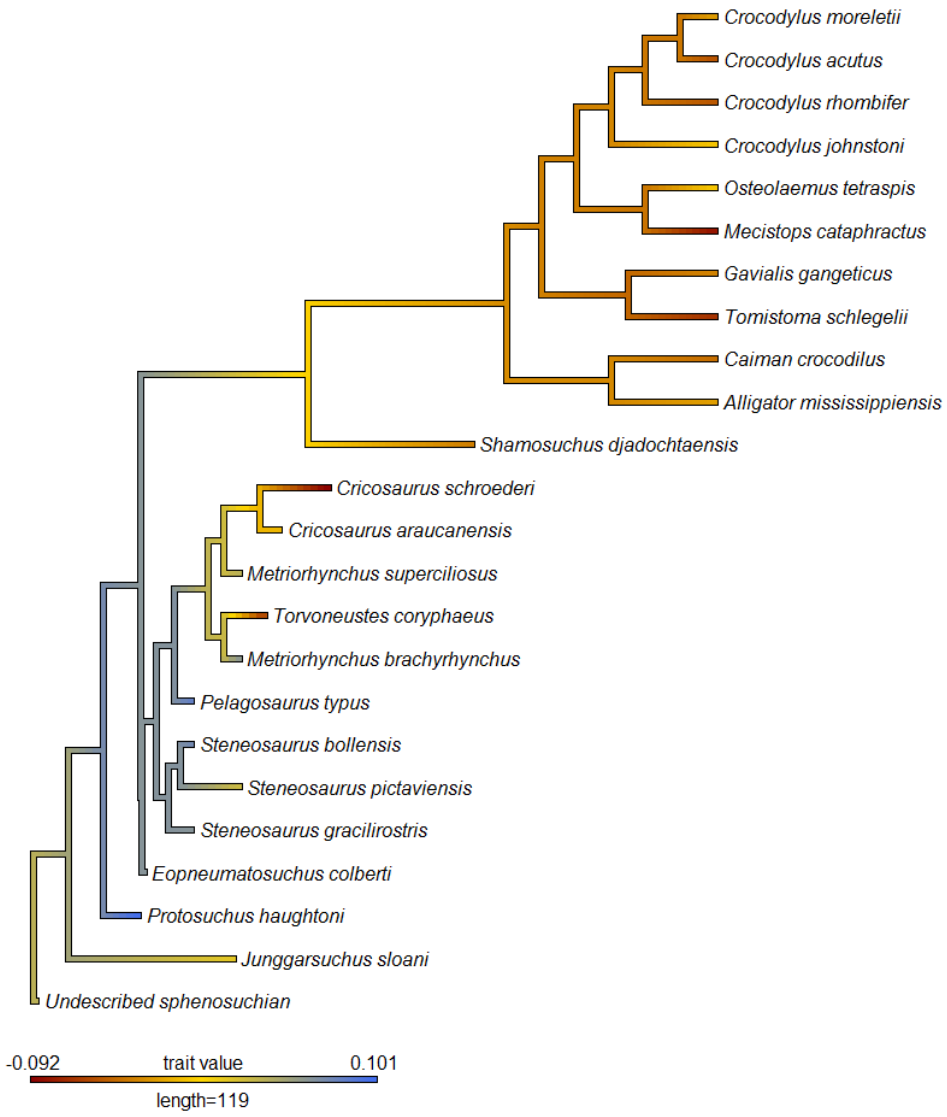


**Fig. S3.** PC2 scores optimized on our primary phylogeny to predict ancestral states for the major clades and assess evolutionary trends.

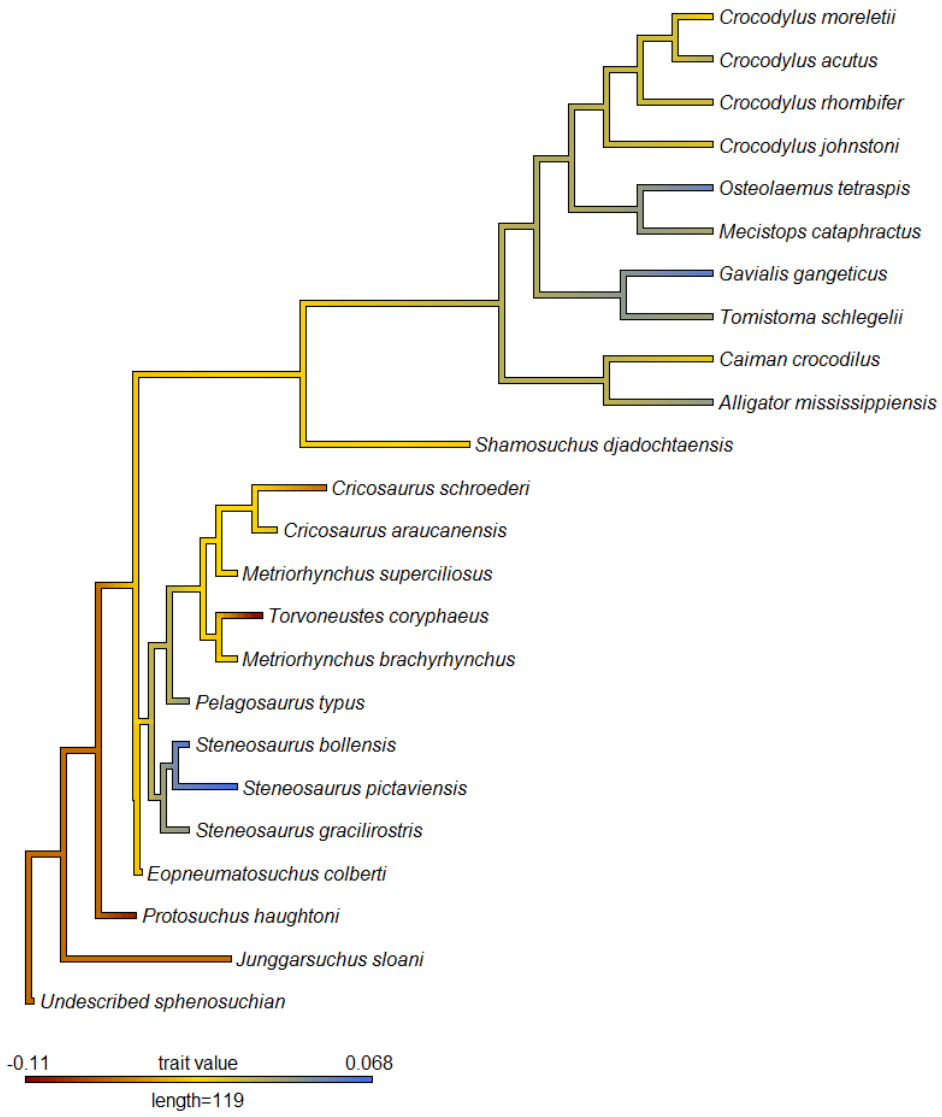


**Fig. S4.** PC3 scores optimized on our primary phylogeny to predict ancestral states for the major clades and assess evolutionary trends.

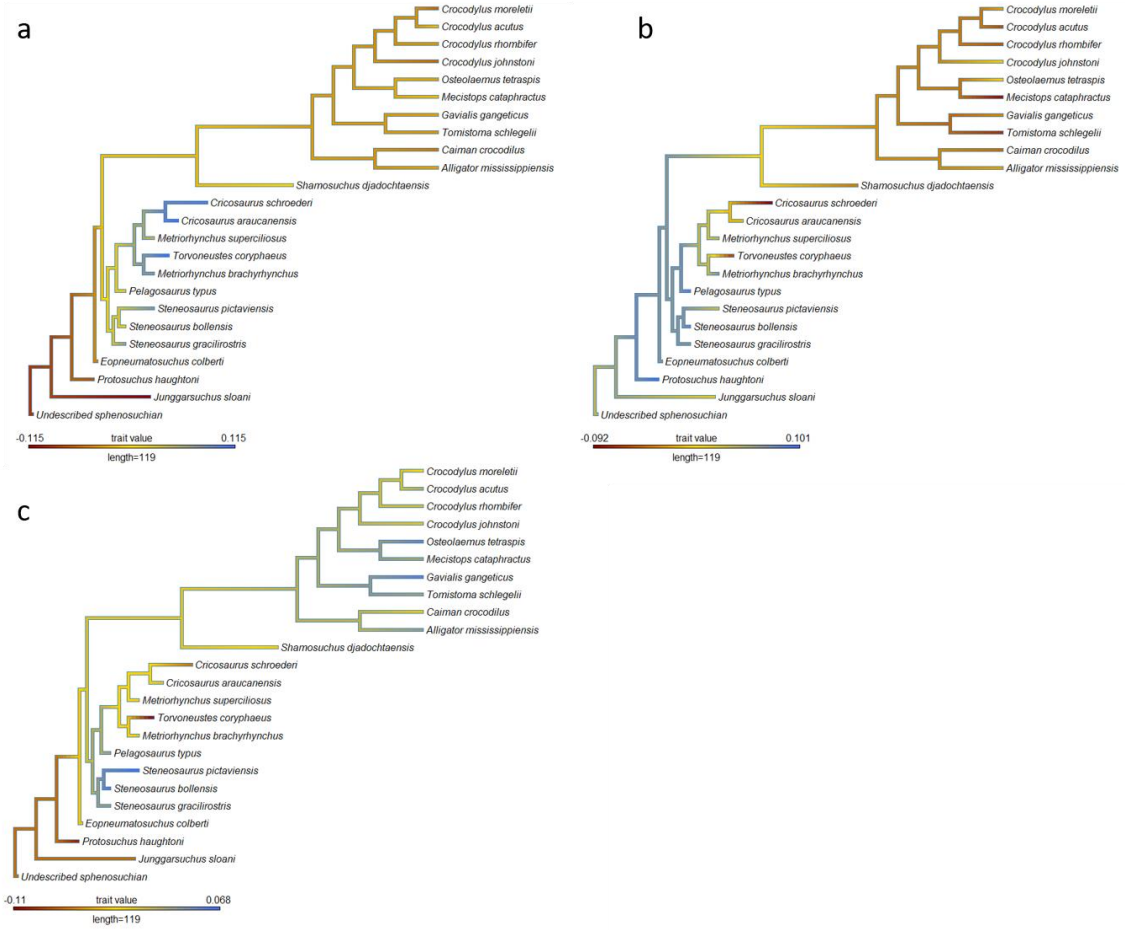


**Fig. S5.** PC scores of the first three principal components, optimized on the phylogeny with *Eopneumatosuchus colberti* placed as the sister taxon to Thalattosuchia + (*Shamosuchus* + Crocodylia), to predict ancestral states for the major clades and assess evolutionary trends. a, PC1; b, PC2; c, PC3.

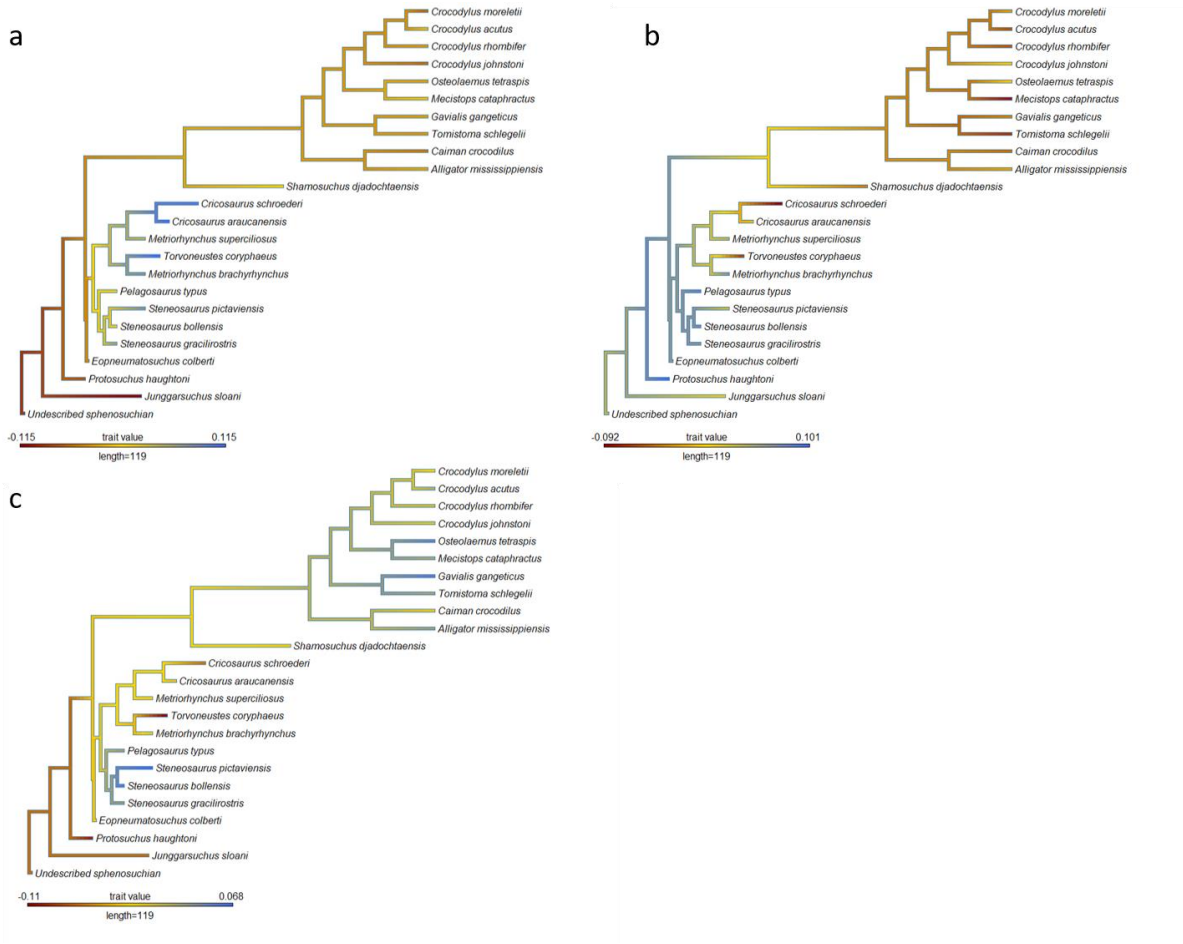


**Fig. S6.** PC3 scores optimized on the phylogeny with *Pelagosaurus typus* positioned as a teleosauroid, to predict ancestral states for the major clades and assess evolutionary trends. a, PC1; b, PC2; c, PC3.

## 10. Evolutionary model fitting

**Table S10.** Five standard models fitted on the first three principal component axes showing the AIC scores. The models are: BM (Brownian motion), OU (Ornstein-Uhlenbeck), EB (Early-burst), trend (Brownian motion with trend) and lambda (Pagel).

**Primary phylogeny**

| | BM | OU | EB | trend | lambda |
|---|---|---|---|---|---|
| **PC1** | -74.485 | -71.856 | -79.996 | -63.232 | -71.856 |
| **PC2** | -69.521 | -68.680 | -69.084 | -64.574 | -67.822 |
| **PC3** | -74.591 | -73.483 | -78.519 | -64.725 | -71.962 |

**Primary phylogeny (fossil specimens only)**

| | BM | OU | EB | trend | lambda |
|---|---|---|---|---|---|
| **PC1** | -36.607 | -33.298 | -33.297 | -39.191 | -33.305 |
| **PC2** | -35.977 | -34.494 | -32.667 | -38.418 | -33.666 |
| **PC3** | -42.606 | -40.841 | -39.524 | -36.884 | -39.297 |

***Eopneumatosuchus colberti* placed as the sister taxon to Thalattosuchia + (*Shamosuchus* + Crocodylia)**

| | BM | OU | EB | trend | lambda |
|---|---|---|---|---|---|
| **PC1** | -72.911 | -70.283 | -78.911 | -61.215 | -70.283 |
| **PC2** | -72.719 | -71.107 | -71.698 | -67.207 | -70.091 |
| **PC3** | -78.059 | -76.365 | -80.978 | -67.787 | -75.429 |

***Pelagosaurus typus* positioned as a teleosauroid**

| | BM | OU | EB | trend | lambda |
|---|---|---|---|---|---|
| **PC1** | -76.211 | -73.582 | -81.262 | -65.216 | -73.582 |
| **PC2** | -69.629 | -68.789 | -69.289 | -64.601 | -67.825 |
| **PC3** | -75.373 | -74.759 | -79.190 | -65.683 | -72.745 |

## 11. Evolutionary rates

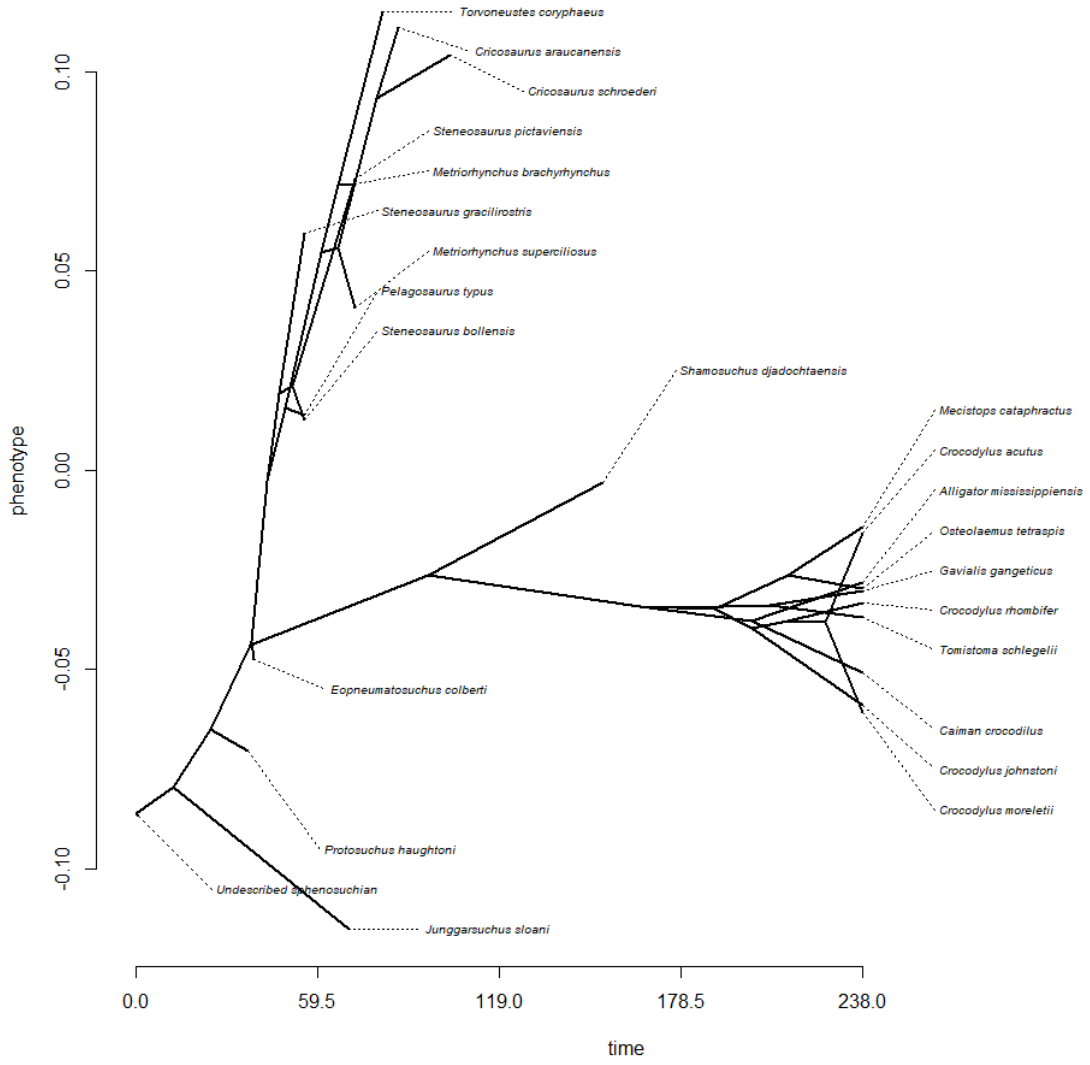


**Fig. S7.** The primary phylogeny is plotted such that the x-axis is scaled to time and the y-axis to PC1 score.

## 12. Cochlear measurements

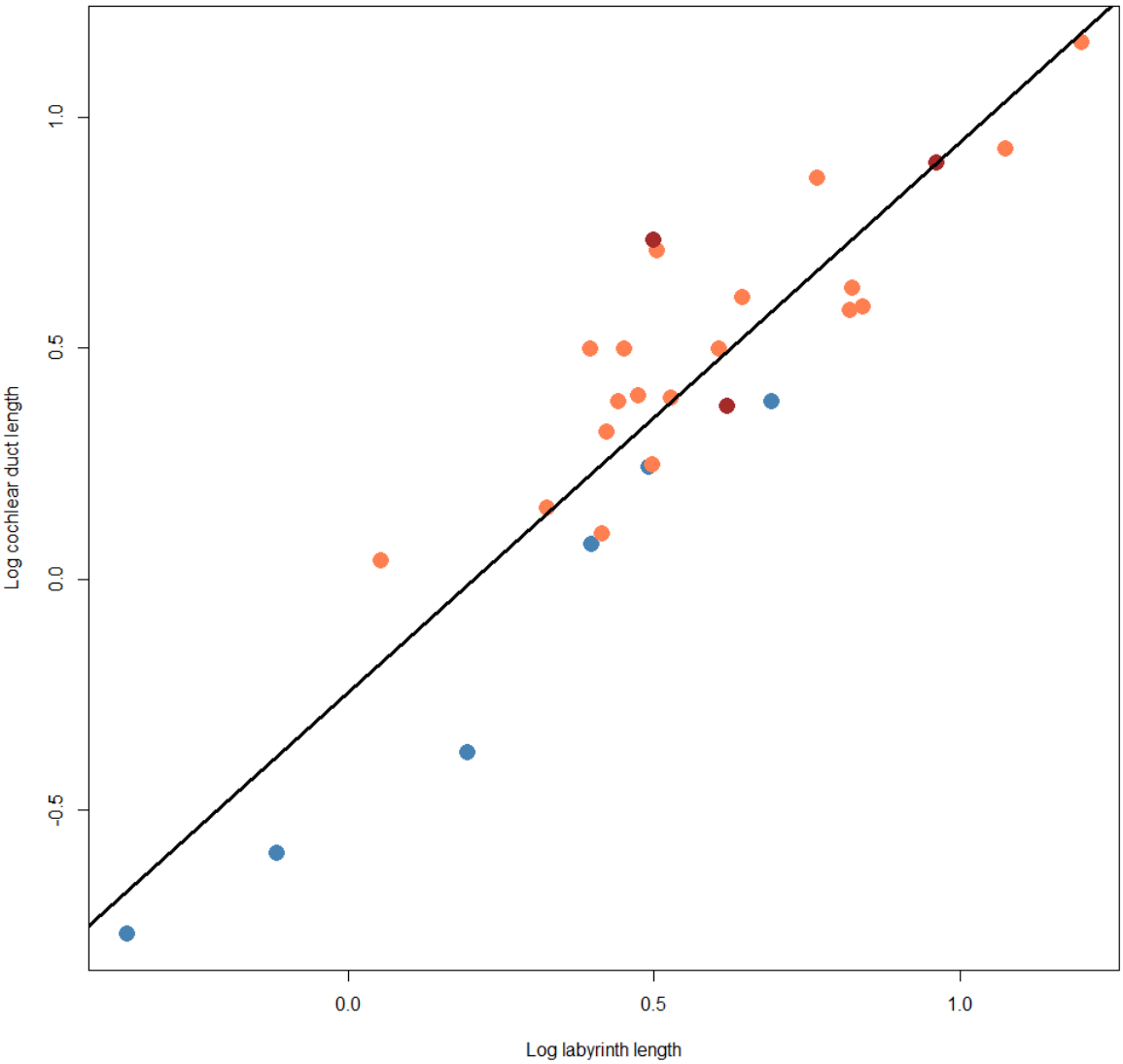


**Fig. S8.** Logarithmic plot of labyrinth length and cochlear duct length. Blue, pelagic; orange, semiaquatic; red, terrestrial.

## 13. Inclusion of *Crocodylus porosus* juvenile

The extant crocodylian *Crocodylus porosus* often ventures further offshore than other extant species. We do not include *C*. *porosus* in our dataset as the scan we acquired is of a juvenile, and we are limiting our analysis to adults. However, to demonstrate that *C*. *porosus* has an inner ear that is similar in shape to other extant crocodylians, and distinct in shape from pelagic extinct thalattosuchians, we provide an auxiliary analysis in which this juvenile specimen is included in our PCA morphospace below (analysis conducted following the same protocol as our primary PCA analysis, described above and in the main text). This demonstrates that the exclusion of *C*. *porosus* should not greatly affect our results, as its ear is exceedingly similar to the many other extant crocodylians in our dataset. We also acknowledge that extant species other than *C*. *porosus* are frequently encountered in brackish or saline environments, including one of the species in our analysis, *C*. *acutus*, and that swimming behavior in extant crocodylians appears to be the same whether an individual is in fresh or salt water. Hence, we wouldn't expect substantial differences in inner ear morphology between coastal and fluviolacustrine extant forms.

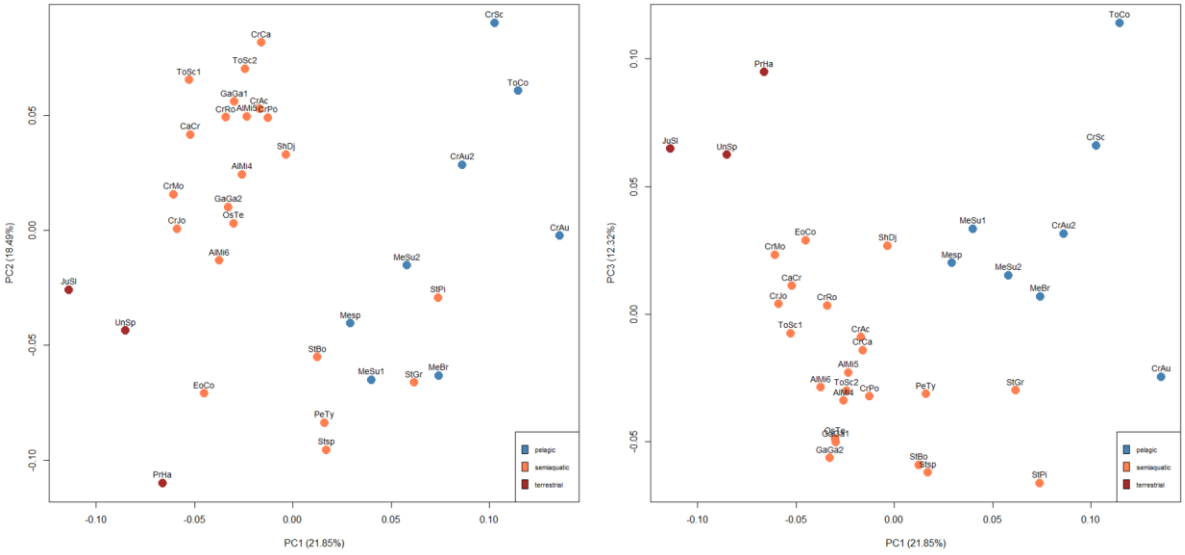


**Fig. S9.** PCA including the juvenile *Crocodylus porosus* (OUVC:10899; CrPo).

## 14. Left-Right Ear Asymmetry

To our knowledge, the only study testing whether left and right inner ear labyrinths of an archosaur are consistent in shape is a recent study of wild turkeys (24). The analyses in our paper use right labyrinths or mirrored left labyrinths. We here test whether mirrored left labyrinths resemble the shape of the right labyrinths in individuals of three key extant species, one from each major crocodilian subgroup. Importantly, we find that, for each individual, the mirrored left and actual right labyrinths fall out very close to each other in PCA morphospace (Fig. S10, analysis conducted following the same protocol as our primary PCA analysis, described above and in the main text), demonstrating that any asymmetry between left and right sides is minimal compared to the much greater amount of variation between species and between habitat groups. Thus, the inclusion of both right and mirrored left labyrinths in our dataset should not provide any serious bias. We visually show the actual left and right labyrinths of the three extant individuals in Fig. S11, which further demonstrates how similar in shape they are.

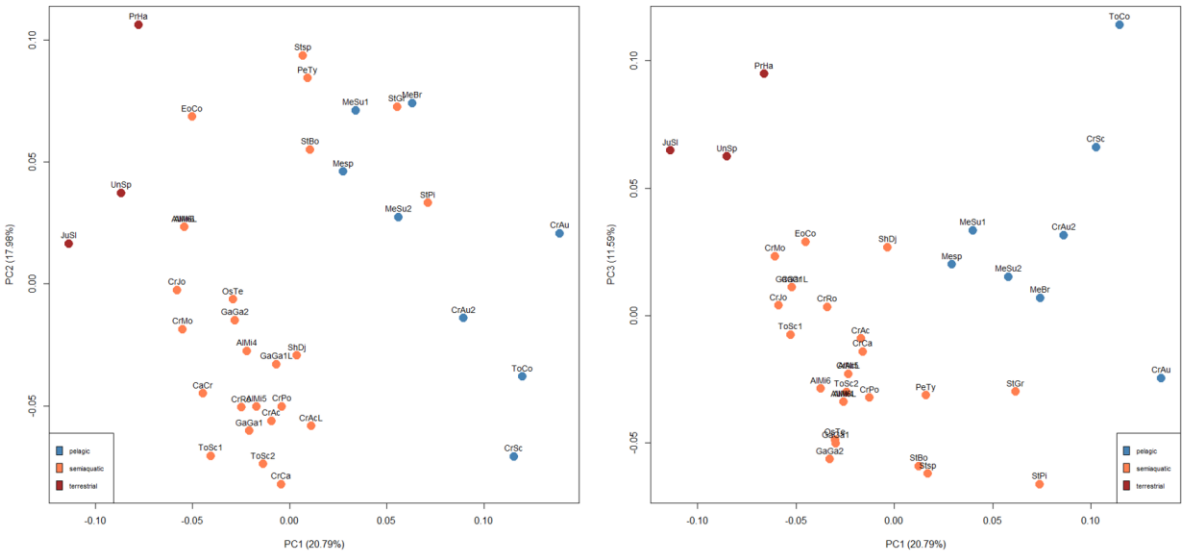


**Fig. S10.** PCA including the left mirrored labyrinths *for Alligator mississippiensis* (OUVC 9761; AlMi6L), *Crocodylus acutus* (FMNH 59071; CrAcL) and *Gavialis gangeticus* (TMM M-5490; GaGa1L).

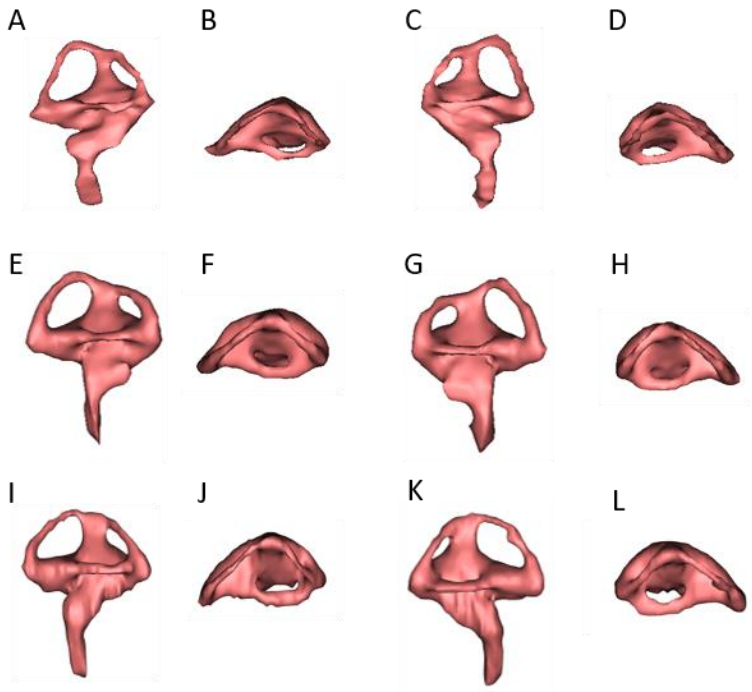


**Fig. S11.** Bony labyrinths of *Alligator mississippiensis* (OUVC 9761), *Crocodylus acutus* (FMNH 59071) and *Gavialis gangeticus* (TMM M-5490). A, E, I left lateral view; B, F, J left dorsal view; C, G, K right lateral view; D, H, L right dorsal view.

## 15. Supplementary References


1. J. M. Clark, X. Xu, C. A. Forster, Y. Wang, A Middle Jurassic ‘sphenosuchian’from China and the origin of thecrocodylian skull. *Nature* **430**, 1021–1024 (2004).

2. A. W. Crompton, K. K . Smith, “A new genus and species of crocodilian from the Kayenta Formation (Late Triassic?) of Northern Arizona” in Aspects of Vertebrate History, L. L. Jacobs, Eds. (Museum of Northern Arizona Press, Flagstaff, 1980) pp. 193–217.

3. E. H. Colbert, C. C. Mook, The Ancestral crocodilian *Protosuchus*. *Bull. Am. Mus. Nat. Hist.* **97**, 143–182 (1951).

4. F. Westphal, Die Krokodilier des Deutschen und Englischen oberen Lias. *Palaeontographica* A 116, 23–118 (1962).

5. C. W. Andrews, Descriptive Catalogue of the Marine Reptiles of the Oxford Clay: Part II (British Museum (Natural History), London, 1913).

6. Y. Herrera, M. Fernández, J. A. Varela, Morfología del miembro anterior de Geosaurus araucanensis Gasparini y Dellapé, 1976 (Crocodyliformes: Thalattosuchia). *Ameghiniana* **46**, 657–667 (2009).

7. Y. Herrera, M. S. Fernández, Z. Gasparini, Postcranial skeleton of *Cricosaurus araucanensis* (Crocodyliformes: Thalattosuchia): morphology and palaeobiological insights. *Alcheringa* ***37***, 1–14 (2013).

8. H. Karl, E. Gröning, C. Brauckmann, N. Knötschke, Revision of the genus *Enaliosuchus* Koken, 1883 (Archosauromorpha: Metriorhynchidae) from the

Early Cretaceous of northwestern Germany. *Studia Geológica Salmanticensia* **42**, 49–59 (2006).

9. M. T. Young, M.B. Andrade, S. Etches, B. L. Beatty, A new metriorhynchid crocodylomorph from the Lower Kimmeridge Clay Formation (Late Jurassic) of England, with implications for the evolution of dermatocranium ornamentation in Geosaurini. *Zool. J. Linn. Soc.* **169**, 820–848 (2013).

10. D. Pol, A. H. Turner, M. A. Norell, Morphology of the Late Cretaceous Crocodylomorph *Shamosuchus djadochtaensis* and a Discussion of Neosuchian Phylogeny as Related to the Origin of Eusuchia. *Bull. Am. Mus. Nat. Hist.* **324**, 1–103 (2009).

11. G. Grigg, D. Kirshner, *Biology and Evolution of Crocodylians* (CSIRO and Cornell University Press, 2015).

12. M. T. Young, *et al*., Convergent evolution and possible constraint in the posterodorsal retraction of the external nares in pelagic crocodylomorphs. *Zool. J. Linn. Soc.* (In press).

13. J. Ristevski, M. T. Young, M. B. Andrade, A. K. Hastings, A new species of *Anteophthalmosuchus* (Crocodylomorpha, Goniopholididae) from the Lower Cretaceous of the Isle of Wight, United Kingdom, and a review of the genus. *Cretac. Res.* **84**, 340–383 (2018).

14. A. Ősi, M. T. Young, A. Galácz, M. Rabi, A new large-bodied thalattosuchian crocodyliform from the Lower Jurassic (Toarcian) of Hungary, with further evidence of the mosaic acquisition of marine adaptations in Metriorhynchoidea. *PeerJ* **6**, e4668 (2018).

15. D. Foffa, M. M. Johnson, M. T. Young, L. Steel, S. L. Brusatte, A revision of the deep-water teleosauroid crocodylomorph *Teleosaurus megarhinus* Hulke, 1871 from the Kimmeridge Clay Formation (Late Jurassic) of England, UK. *PeerJ* **7**, e6646 (2019).

16. M. M. Johnson, M. T. Young, S. L. Brusatte, Re-description of two contemporaneous mesorostrine teleosauroids (Crocodylomorpha, Thalattosuchia) from the Bathonian of England, and insights into the early evolution of Machimosaurini. *Zoo. J. Linn. Soc.* zlz037 (2019).

17. S. Sachs, M. T. Young, P. Abel, H. Mallison, A new species of *Cricosaurus* (Thalattosuchia, Metriorhynchidae) from the Upper Jurassic of southern Germany. *Acta Palaeontologica Polonica* **64**, 345–356 (2019).

18. E. W. Wilber, What's in an Outgroup? The Impact of Outgroup Choice on the Phylogenetic Position of Thalattosuchia (Crocodylomorpha) and the Origin of Crocodyliformes. *Syst. Biol.* **64**, 624–637 (2015a).

19. E. W. Wilber, A new metriorhynchoid (Crocodylomorpha, Thalattosuchia) from the Middle Jurassic of Oregon and the evolutionary timing of marine adaptations in thalattosuchian crocodylomorphs. *J. Vert. Paleo.* 902846 (2015b).

20. E. Buffetaut, Position systématique et phylogénetique du genre Pelagosaurus Bronn, 1841 (Crocodylia, Mesosuchia), du Toarcian d'Europe. Geobios 13, 783–786 (1980).

21. J. R. Oaks, A time-calibrated species tree of crocodylia reveals a recent radiation of the true crocodiles. *Evolution* **65**, 3285–3297 (2011).

22. J. Harshman, C. J. Huddleston, J. P. Bollback, T. J. Parsons, M. J. Braun True and false gharials: a nuclear gene phylogeny of crocodylia. *Syst Biol* **52**, 386–402 (2003).

23. M. S. Y. Lee, A. M. Yates Tip-dating and homoplasy: reconciling the shallow molecular divergences of modern gharials with their long fossil record. *Proc. R. Soc*. *B* **285**, 20181071 (2018).

24. D. G. Cerio, L. M. Witmer, Intraspecific variation and symmetry of the inner-ear labyrinth in a population of wild turkeys: implications for paleontological reconstructions. PeerJ 7, e7355 (2019).